GeoJournal 17.4 545–568

Topography as a Fundamental Element of Glacial Systems

A New Approach to ELA* Calculation and Typological Classification of Paleo- and Recent Glaciations

Kuhle, Matthias, Prof., Dr., University of Göttingen, Institute of Geography, Goldschmidtstraße 5, D-3400 Göttingen, FR Germany

ABSTRACT: The equilibrium line of glaciers as a climate-sensitive parameter is indispensable for the assessment of changes in climate through time. The methods previously developed for calculating the equilibrium line do not obtain, however, satisfactory accuracy. Using the statistical evaluation of data collected from 223 glaciers it is shown here that the inaccuracy of the prevailing methods generally results from the negligence of the specific glacier geometry.

In calculating realistic ELAs glaciers must be understood as dynamic systems whose variables, climatic environment and topography, are linked through feedback. The accompanying transformation in this dynamic system, which is expressed by the difference between a mathematical index and the ELA, can be exactly determined with a regression line. The climatically induced change in glacier geometry is the controlling factor, i.e. operator. The behavior of glacial systems in view of long-term climatic variations can first be understood when the details of the interdependency between topographical and climatic parameters are fully known, as will be demonstrated here.

Introduction

The glaciation of continents, its variability in time and space, and the associated climatic implications have long been an object of research: J. Walcher (1773) was the first to attribute changes in glaciers to climatic variations. Subsequently, several attempts were made to calculate a specific index by means of abstraction from the absolute size and configuration of glaciers. From the location of this glacier-index and its change over time it may be possible to draw direct conclusions as to the climatic conditions. First developed by Simony, Brückner, Richter, Kurowski, Finsterwalder and v. Höfer all such methods were derived on the basis of relatively little experience gained under temporal restrictions in spatially limited areas, using glaciers of the E and W Alps as examples. The technique of specific mass budget measurement developed by H. W. Ahlmann (1948) since the 1920s and the expansion of glaciological research to glaciations outside Alpine areas, especially during the "International Hydrological Decade" (IHD, 1963–1973), as well as the publication of large scale maps of glaciers from all parts of the world provide us with a broad empirical basis to reexamine the suitability of these methods. In this context two aspects have to be considered in more detail: (1) to be of climatic significance it must be ensured that the method for determining a specific glacier index is independent with regard to the actual dimensions and geometric configuration (type) of the glaciers, (2) to be usable for paleoclimatic research the calculation method must be applicable to both former and recent glaciers with the same accuracy[1)].

* ELA = Equilibrium Line Altitude

1) In previous studies concerning methods of ELA assessment (Gross et al. 1977; Braithwaite & Müller 1980; Hawkins 1985), for example, the applicability to various types of glaciers was not reflected. This was caused by the fact that nearly all examples given were of the firn basin type (cf. Fig 6). However, it was indicated that both piedmont glaciers and ice caps (Meier & Post 1962, 70) as well as avalanche caldron glaciers (Müller 1980, 82) have area ratios which differ significantly from those of the firn basin type.

Prevailing Methods of Determining Glacier Indexes

An initial approach to a specific glacier index was the "summit method" which F. Simony (acc. Drygalski & Machatschek 1942, 11) and subsequently Partsch (1882) and Brückner (1887) applied to the subrecent glaciers of the Alps. In this case, the average difference in elevation between glacier-free and perpetually firn- or glacier-covered summits is calculated. Enquist (1916) designated this as the "glaciation limit". Although this method is still being used for recent glaciers (Østrem 1966; Andrews & Miller 1972), reliable values for subrecent glaciations are not obtained. In the critical boundary zone between glaciated and unglaciated summits glacial erosion and accumulation is least distinct due to quantitative and temporal reasons and undergoes the greatest postglacial change as well. Thus, glacial evidence in the boundary zone of a former glaciation is least likely to be preserved. In addition, the climatic significance of the "glaciation limit" and its relationship to the ELA (= Equilibrium Line Altitude, i.e. the line, where ablation equals the accumulation is not yet sufficiently proven since the glaciation of summits) is greatly influenced by local topography (Andrews 1975, 49). Reliable indications of a former glaciation are, contrarily, accumulations and erosional features of ice bodies which originated in the zone of optimal glaciation. This is accounted for best by the area ratio method developed by E. Brückner (1886) and E. Richter (1888) using glaciers of the E Alps as examples. According to this method it is assumed that the zones of accumulation and ablation of a glacier have an areal ratio of 3:1 and that the resulting line separating the two represents the approximated value of the equilibrium line (in Brückner = firn line). Kurowski (1981) on the other hand, equates the area-weighted mean altitude of a glacier with its ELA (here named the snowline, however used in the modern sense of ELA), whereby he postulates that ablation and accumulation are linear functions of altitude above sealevel. R. Finsterwalder (1953) assumed that the relationship of oblation and accumulation to altitude is parabolic in calculating its ELA.

These methods were based more or less on theoretically fixed conditions for glacier mass budget because quantitative data necessary for an inductive method were not yet available. However, with the increasing information on specific mass and energy budgets of glaciers it became clear that the equilibrium line of a glacier represents a system in which several climatic factors are integrated. For example, the local variability of glacier indexes (cf. Andrews 1975, 21–28) shows that the climatic parameters constituent for glacier formation are not rigidly quantitatively fixed but are variable due to possible mutual compensation. An exact determination of the ELA is thus only possible by using the direct glaciological method (Ahlmann 1948), which is, however, limited to a few exemplary cases due to the great expenditure of work required (e.g. Storglaciaeren, Schytt 1962; South Cascade Glacier, Meier & Tangborn 1965; Hintereisferner, Hoinkes 1970). In addition, this method is only applicable to recent glacier systems. This is true as well for the method of Lichtenecker (1938) and Visser (1938), which is also based on mass budget and assumes that the ELA lies in the zone of the highest lateral and medial moraines. This method yields excellent approximated values for recent and subrecent stades (Andrews, 1975, 54 f. Gross et al. 1977; Müller 1980). However it is not applicable to older phases of glaciation because lateral moraines of maximum alpine glaciations are always deposited on steep slopes subject to undercutting, i.e. the preservation of the highest glacial residuals is contingent upon relief and thus random (cf. Hawkins 1985).

Based on the voluminous quantitative glaciological data currently available (cf. Kasser 1967, 1973; Müller 1977) a promising study, in imitation of Brückner's method (1886), was made on the relationship between the mass balances of glaciers and the AAR (Accumulation Area Ratio, i.e. ratio between accumulation area and total glacier surface) with the aim of calculating the ELA for glaciers whose specific mass balances are unknown. Studies by Meier and Post (1962) on 475 North American glaciers yielded an AAR range of 0.5 to 0.8 for glaciers with balanced regimes. However, it must be taken into account here that the South Cascade Glacier, for example, with an AAR value of 0.58 has a specific net budget of zero (Meier & Post 1962, 70), while the Hintereisferner (Ötztaler Alps) with the same AAR of 0.58 (1952/53 to 1963/64, Hoinkes 1970, 59) has a negative net budget ($b = -48.06$ g/cm^2), resulting in a retreat of 27.3 m/yr (1959/60 to 1970, Kasser 1967, 1973; Müller 1977). The neighbouring Kesselwandferner with a steep crevassed tongue, on the contrary, has an AAR of 0.8 and a balanced regime (Gross et al. 1977, 232). Thus the area ratios of 0.5 to 0.8 only denote the range within which there is only one specific value at which a glacier attains a net budget of zero. In the case of the Hintereisferner an AAR between 0.5 and 0.8 signifies however a possible range in ELA of 250 m when the glacier only has a total vertical extension of 1238 m! Gross et al. (1977) consider an AAR of 0.67 (derived from eight selected Alpine firn basin glaciers) as a constant value for stationary glaciers. Wang Yinsheng et al. (1983, 23, Tab 6) calculated Sc/Sa (ablation area/accumulation area) surface ratios between 1:0.6 and 1:1.3, i.e. AAR values of 0.39 to 0.56, for glaciers of the E Tian Shan (Mt. Bogda region). Müller (1980, Tab 2) determined an average AAR of 0.41 ± 0.19 (0.37 ± 0.13 for valley glaciers only) in the Mt. Everest region. On a scale of 0.37 to 0.8 for valley glaciers the ratio of accumulation to total surface area does not prove to be generally predictable. ELAs derived from an assumed AAR of 0.6 ± 0.1 (Andrews 1975; Gross et al. 1977; Porter 1981; Hawkins 1985) can thus be regarded as rough approximated values and are only of limited climatic significance. The cause for this must be the lack

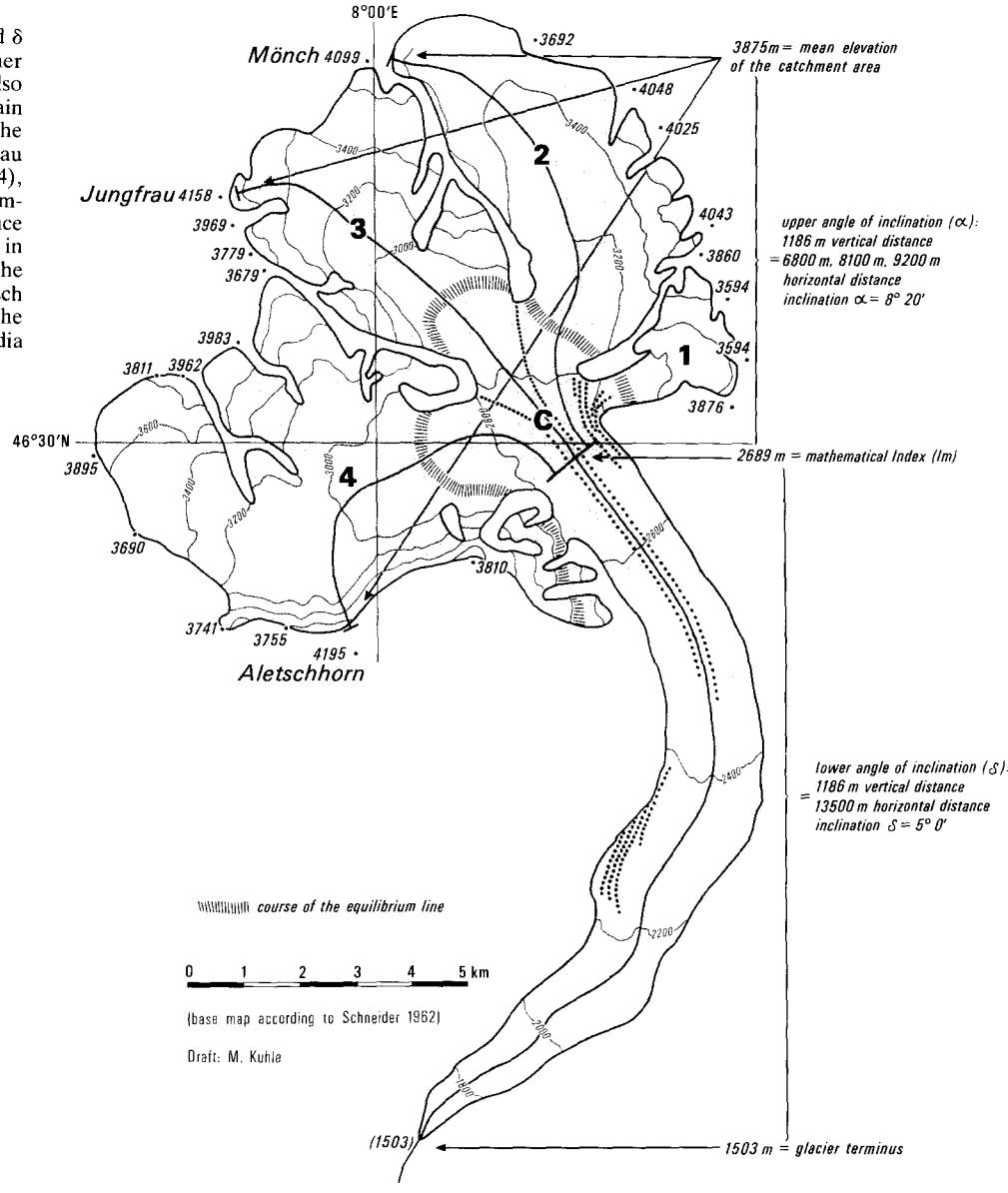

Fig 1
Determination of the angles α and δ using the Aletsch glacier (Berner Oberland, Switzerland; see also cross-section, Fig 2a). The main catchment area is formed by the Ewigschneefeld (2), the Jungfrau firn (3) and the large Aletsch firn (4), while the Grunegg firn (1) is of comparatively subordinate importance for nourishment and thus not used in the calculation of the angle α; the same is true for the middle Aletsch glacier (5) which does not reach the main valley glacier C: Concordia place

of a variable, the neglect of which gives rise to the unpredictable variation in the AAR values.

One factor essential to the formation of glaciers is topography which is, however, ignored in area ratio calculations. Müller (1980, 82) attributed the extremely low AAR values in the Mt. Everest region with an average of 0.41 to the topographical setting and the resulting specific type of nourishment (in the Mt. Everest region avalanche and firn caldron glaciers with secondary nourishment are prevalent, cf. Fig 6). Gross et al. (1977) excluded those glaciers surrounded by high backwalls and with sharp breaks in slope from their comparative studies because unpredictable deviations in the area ratio are the rule in such cases.

In case of specific mass balances, which treat glaciers as climate- (not topography-) controlled equilibrium systems, the influence of the topographical setting is expressed only indirectly in the path of the curve for the specific mass balance (e.g. reduction in the positive balance in the area of the surrounding backwall; wind redistribution of snow; see also Young 1975). When, however, no direct observations are made or possible and a rigid mathematical method is used for the assessment of the ELA, it must be assured that the calculation is not affected by the distorting influence of topographic controls. A fundamental change in the topographical setting of a glacier, i.e. in the glacier geometry and type of nourishment (see Fig 6), is often connected with the transition from the former to recent glaciation of a region. In the Tibetan Himalayas, for example, the type of glaciation changed from recent avalanche and firn caldron glaciers to an ice stream system (Kuhle 1982, 1987), i.e. from predominantly secondary avalanche nourishment to primary snow accumulation. Hence, the

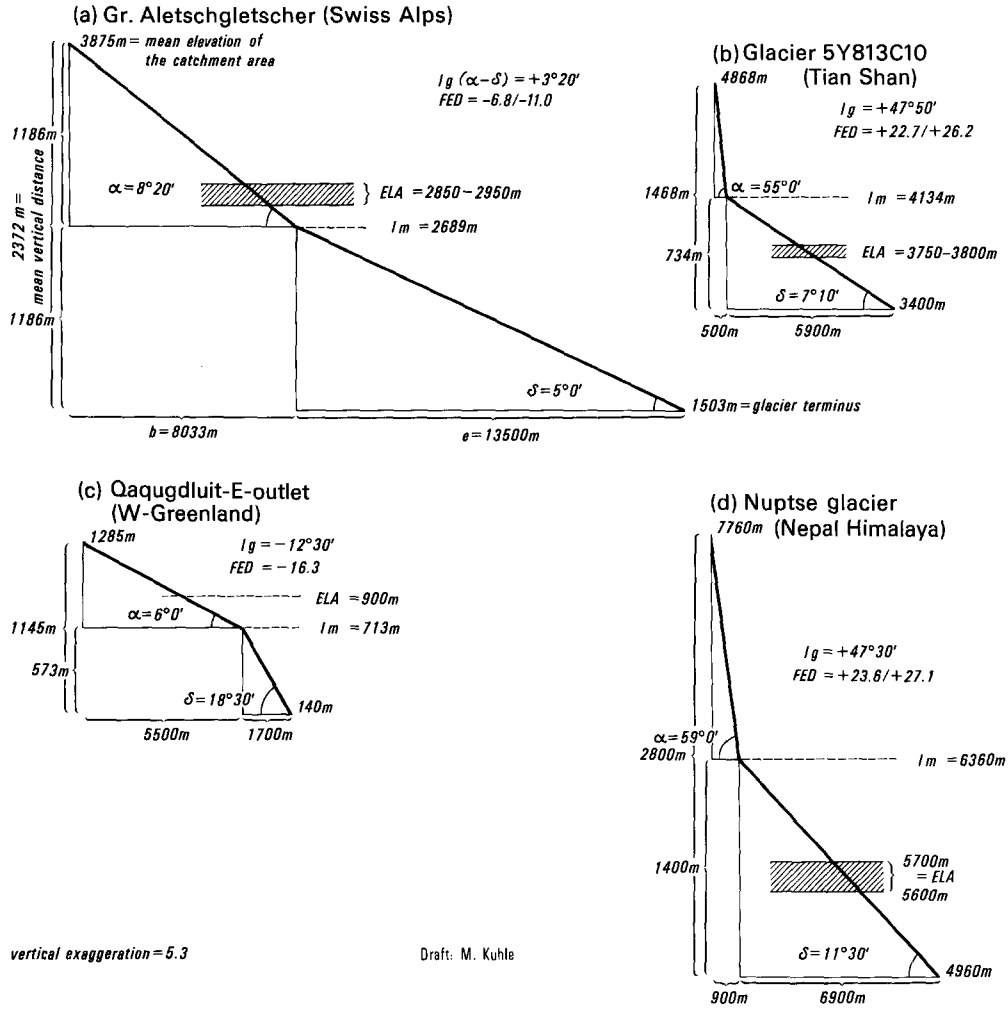

Fig 2
Diagram of exemplary angle differences (I_g) and equilibrium line deviations (FED) of modern glaciers

deduction of the area ratios of more extensive subrecent glacier stades based on the area ratios of recent glaciers from the same region is impermissible in case the area ratios are dependent upon the type of glacier. In addition, the inferred area-elevation curves and thus the ELA values can be considerably different for the same glacier outline through ambivalent reconstructions of the surface contours for paleo-ice bodies (Hawkins 1985, 208). Consequently, the AAR method does conflict with both of the criteria for glacier index assessment given at the beginning.

In the first instance, only the glacier outline, i.e., topographical data, can be inferred from subrecent glaciers, whereas the accompanying climatic parameters represent the desired unknown quantity. Only through the elimination of the influence which the topography has on glaciers is it possible here to determine a purely climate dependent index which approximately corresponds to the ELA. Also applying the method of v. Höfer (1879), which is recommended by UNESCO/IASH (1970 a) and uses the mathematical mean between the average altitude of the catchment area and the glacier terminus, both factors are mixed so that the resulting shifts in the ELA do not only reveal climatic changes but changes in glacier geometry as well. To clear up these methodical uncertainties and to guarantee the interpretability of the calculated ELAs as climatic indexes, the relationship between topography and glacier behavior must be completely understood.

Conception of the Factor of Equilibrium Line Deviation (FED)

To check and quantify the dependency of the ELA on glacier geometry a method was developed which (a) yields a glacier-specific mathematical index having the same accuracy for both recent and former glaciers, (b) depicts glacier geometry with its fundamental elements, and (c) clarifies the interdependency between the geometric index, mathematical index, and ELA via a suitable statistical analysis.

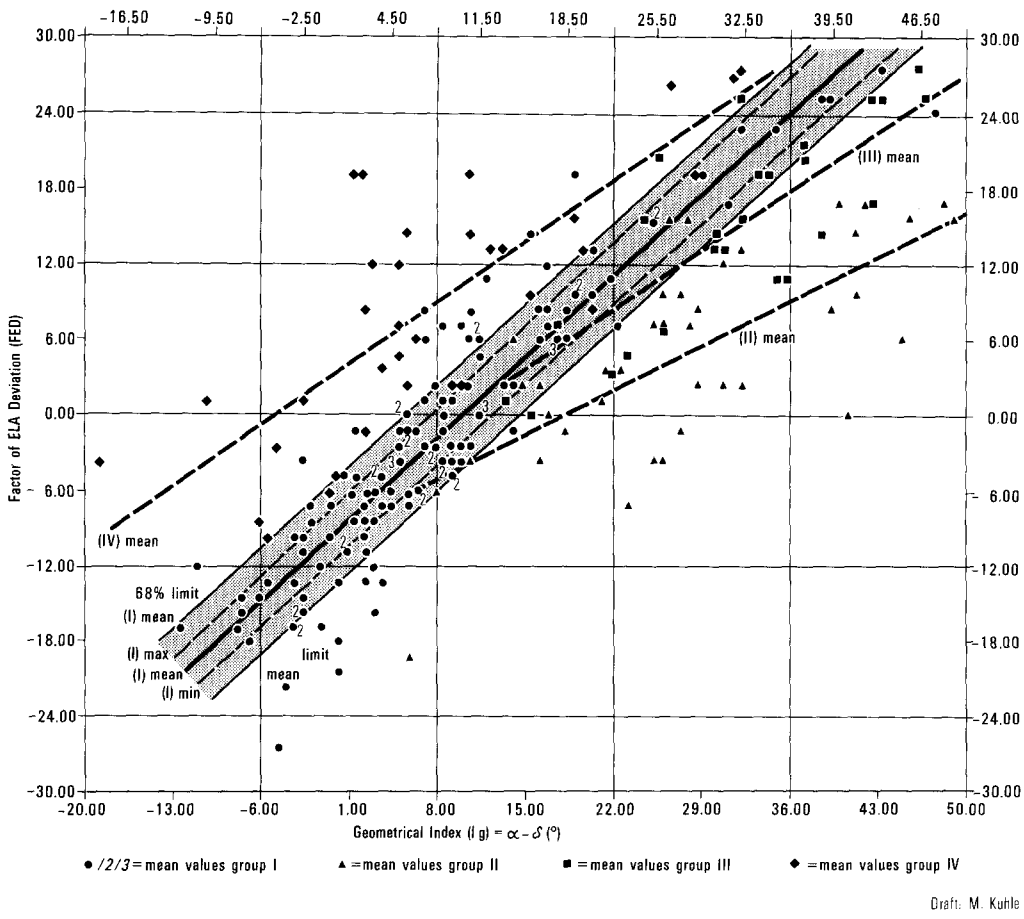

Fig 3
Regression lines I, II, III and IV in the scatter diagram of the mean values for groups I–IV (Tab 1, col. 11+12)

(a) Mathematical index (I_m)

The method of determining a mathematical index is based on two quantities which can be determined for both former and recent glaciers with the same accuracy. First, the average summit elevation above a base value is calculated. The base value is a rough approximation of the ELA determined with the calculated mean between the highest backwall elevation and the glacier terminus

$$(= \frac{\text{highest summit of catchment area (m asl)} - \text{terminus (m asl)}}{2} + \text{terminus (m asl)}).$$

Only the major summits of the catchment area (i.e. no points from continuous ridges) or in the case of plateau glaciers the highest points on the ice surface which lie above the base value will be regarded for the calculation of the average summit elevation. (In rare cases, the base value can lie too high, i.e. higher than the summits of a tributary component; e.g., large dendritic glaciers extending over great distances which have variations in ELA and whose individual catchment areas have very differing altitudes. For instance, the primary base value for the Muldrow glacier (Mt. McKinley) is 3554 m, so that the surrounding ridge of the Brooks glacier would be cancelled out for the most part. In this case, the mean must be calculated from all three main components, i.e. the Muldrow, Traleika and Brook glaciers, to be 3193 m). The mathematical mean calculated with the average summit elevation and the lowest ice margin position is designated in the following as the mathematical index

$$(I_m = \frac{\text{average summit elev. (m asl)} - \text{terminus (m asl)}}{2} + \text{terminus (m asl)}).$$

(b) Equilibrium line altitude (ELA)

The ELA values (Tab 1, col. 8 and 9) were obtained in different ways. For several glaciers they were already available from longterm studies (Kasser 1967, 1973; Müller 1977). These ELAs deviate in part from the values given by Braithwaite and Müller (1980, 265, Tab 1). In such cases, both values were taken into account. Data on direct observations from Swiss glaciers were available (Müller et al. 1976). However, the values given here solely concern 1973 and thus can only be taken as conditionally representative for the corresponding long-term ELA, i.e. they are only used as an informal reference point. Emphasis was rather given to

values obtained with the Lichtenecker method (1938) which agreed very well with the long-term ELA of glaciers determined with specific mass balances (cf. Müller et al. 1976; Gross et al. 1977; Müller 1980). The Lichtenecker method was also applied to all other glaciers for which only a one-year or no direct observation was made. There were, in part, great deviations in the ELA values especially for compound glaciers facing different directions. In these cases, minimum and maximum values were given.

(c) Geometrical index (Ig) and the factor of equilibrium line deviation (FED)

The next step was the attempt to discover a regular relationship between the mathematical index and the ELA. The initial idea here was that the mathematical calculation divides the continuum of a glacier between the level of the summit elevation and the terminus into two halves, taking only the vertical and not the horizontal extension into account. Fundamentally, the separation of an upper, surficially larger catchment area from a lower ablation area, which is surficially smaller due to the conical confluence of the ice, is to be expected. This corresponds to the fact, that in most cases the accumulation area of stationary glaciers is greater than the ablation area. However, the specific topography in which the glacier is formed remains disregarded. Hence, the mathematical index, for example, for a glacier with a high surrounding ridge and a gently inclined tongue would be too high and thus would divide a very steep, surficially underrepresented upper zone with low accumulation and ice formation potential from a level, oversized lower zone. In such a case, the ELA would be lower than I_m (Fig 2b, d). The opposite is true for a gently inclined plateau glaciation with steep outlet glaciers. Using a vertical averaging method the upper zone would be too large in comparison to the lower zone – the mathematical index would then lie below the ELA (Fig 2c). In order to be able to check this hypothesis comparatively, the decisive inclination relationships of the glacier must be represented. With respect to the mathematical index, the horizontal distance parallel to slope in the direction of the highest point of the catchment area, but only to the average summit elevation, is measured from the corresponding contour line on the surface of the glacier (Fig 1). In the case of compound glaciers with several components this procedure is repeated for each of the corresponding catchment areas. (In the case that the highest point of a tributary catchment area does not quite reach the mean summit height, the calculation of the angle must be done with the highest point of the catchment area).

The horizontal from the glacier terminus up to the level of I_m is calculated in the same way. The angles are obtained with the tangent, whereby α denotes the upper angle of inclination and δ the lower (Fig 1 and 2a; Tab 1, col. 4 and 5). The geometrical index (I_g) of a glacier is calculated by $\alpha-\delta$ (Tab 1, col. 6) and is set in relation to the equilibrium line deviation (I_m-ELA). Assuming that the interdependency of angle difference and equilibrium line deviation outlined above does exist, the amount of deviation (I_m-ELA) must act linearly proportional to the vertical distance of the glaciers out of geometrical necessity. In order to eliminate absolute dimensions the factor of equilibrium line deviation (FED; Tab 1, col. 11) is expressed in percent of the vertical:

$$FED = \frac{(I_m - ELA) \cdot 100}{\text{vertical distance}}$$

(d) Distortional effects

In order to reveal the dependency of the ELA deviation on I_g explained in Sect. (c) effects leading to distorted results are specified and named as far as possible.

Steeply breaking off or calving tongues, for example, would have to result in an irregular raising of the mathematical index and thereby in an increase in the amount of deviation (I_m-ELA). In the same way, noncanalized broadly flowing ablation zones (piedmont glaciers) cause the mathematical index to be relatively too high and thereby result in greater equilibrium line deviations. On the other hand, a thick debris cover on the ablation zone helps to preserve the ice mass, i.e. the glacier tongue reaches relatively lower altitudes, whereby the mathematical index is lowered, and the deviation factor decreases. Since this effect would have to be evident in dependency on the relative size of the debris-covered glacier surface, its percentage in relation to the total surface of the ablation zone was first estimated. In doing so, the thickness of the debris cover had to be disregarded. In addition, it can be expected that with very shallowly inclined tongues a cover of 75%, for example, has less of an effect on the amount of deviation than with steeper tongues which only need a short horizontal distance to acquire a greater vertical extension in a shorter time. Thus, it becomes clear that equal percentages of debris cover do not necessarily have to be accompanied by the same change in equilibrium line deviation. As shown with the following correlation, the deviation was not affected in linear proportion to the relative amount of debris cover due to this complexity. However, a general reduction in the amount of deviation can be ascertained for percentages of cover greater than 25%. Therefore, a classification of the degree of cover was abandoned. Distortion of the equilibrium line deviation is likewise to be expected with catchment areas with an average summit height over 7000 m. As telemetric temperature measurements on precipices in the Mt. Everest region have shown (Kuhle 1986b), there are virtually no temperatures above 0° C in ice or rock over 7000–7100 m alt. Thus the zones above 7000–7100 m are, according to the definition of Shumskii (1964, 407), in the recrystallization zone.

Tab 1 Geometrical indexes, mathematical indexes and equilibrium line deviation of modern glaciers*)

1	2	3	4	5	6	7	8	9	10	11	12
A 01	Hintereisferner	Fm	11°50'	6°20'	+ 5°30'	2936	2950–3050	I 2969 1952/53–64/65 E 2995 1955–1964 E 2951 1965–1974 K/N 2972 1952/53–7475 A 2910∓20 1953–1975	1	– 1.1/– 5.2	I
A 02	Kesselwandferner	Fm	9°30'	14°50'	– 5°20'	3047	3100–3150	E 3094 1953–1975	1	– 6.3/–13.0	IV
A 03	Hochjochferner	Fm	17°20'	13°20'	+ 4°00'	2984	3000–3050		1	– 1.7/– 7.0	I
A 04	Langtaufererferner	Fm	18°30'	11°30'	+ 7°00'	2922	2900–3000		1	+ 1.9/– 6.7	I
A 05	Gepatschferner	Fm	7°40'	11°30'	– 3°50'	2720	3000–3050		1	–19.4/–22.9	I
A 06	N Guslarferner	Fm	18°20'	12°20'	+ 6°00'	3064	3050–3080		1	+ 1.9/– 2.2	I
A 07	Taschachferner	Fm	12°30'	16°00'	– 3°30'	2830	3050–3100		1	–14.7/–18.0	I
A 08	Mittelbergferner	Fm	10°30'	17°20'	– 6°50'	2748	2950–3000		1/2	–15.6/–19.5	I
A 09	Marzellferner	Fm	20°20'	10°40'	+ 9°40'	2946	2950–3060		2	– 0.3/– 9.6	I
A 10	Schalfferner	Fm	14°20'	8°40'	+ 5°40'	2937	2950–3050		2	– 1.3/–10.9	I
A 11	Diemferner	Fm	14°20'	10°50'	+ 3°30'	2998	3000–3100		2	– 0.3/–13.1	I
A 12	Gurglerferner	Fm	7°00'	12°30'	– 5°30'	2782	2900–2980		2	–10.1/–17.0	I
A 13	Langtalerferner	Fm	17°20'	7°00'	+10°20'	2896	2850–2950	I/K 2907 1962/63–69/70 E 2878 1963–1970 A 2850∓30 1963–1970	2	+ 5.0/– 1.2	I
A 14	Rotmoosferner	Fm/Fk	24°30'	13°20'	+11°10'	2825	2800–2850		2	+ 2.5/– 2.5	I
A 15	Gaißbergferner	Fm/Fk	26°40'	12°20'	+14°20'	2899	2850–2900		2	+ 5.3/– 0.1	I
A 16a	W Vernagt-ferner 1969	Fm	14°00'	11°50'	+ 2°10'	3055	3050	E 3054 1965–1975 A 3080∓30 1966–1975	3	– 0.7	IV
A 16b	E Vernagt-ferner 1969	Fm	17°50'	11°20'	+ 6°30'	3161	3100–3150	E 3054 1965–1975 A 3080∓30 1966–1975	3	+ 9.2/+ 1.7	IV
A 17	Untersulzbach Kees	Fm	15°10'	11°50'	+ 3°20'	2766	2620	H 2620	4	+11.7	IV
A 18	La Cudera	Fm	18°30'	21°00'	– 2°30'	2821	2850–2900	M 2907 ∅ 1973	5	– 4.4/–11.9	I
A 19	Silvrettagletscher	Fm	25°30'	9°20'	+16°10'	2809	2750–2780	I/K 2784 1960/61–69/70 N 2757 1959/60–74/75 E 2776 1961–1975 A 2760∓30 1960–1975 M 2860 ∅ 1973	5	+ 7.8/+ 3.8	I

Tab 1 Geometrical indexes, mathematical indexes and equilibrium line deviation of modern glaciers*)

1	2	3	4	5	6	7	8	9	10	11	12
A 20	Ochsentalergl.	Fm	27°50'	18°30'	+ 9°20'	2754	2750–2800		5	+ 0.4/ −5.1	I
A 21	SW Vermunt-gletscher	Fm	22°40'	13°20'	+ 9°20'	2752	2750–2800	M 2840 Ø 1973	5	+ 0.3/− 7.2	I
A 22	Jamtalferner	Fm	22°40'	12°50'	+ 9°50'	2758	2750–2800		5/6	+ 1.0/− 5.4	I
A 23	W Larainferner	Fk	37°30'	15°10'	+22°20'	2822	2720–2750		6	+13.0/+ 9.2	I
A 24	Vedretta di Scersen Inferiore	Fm	29°00'	9°30'	+19°30'	2950	2750–2800		7	+17.6/+13.2	IV
A 25	Vedretta di Scersen Superiore	Fm/Fk	32°00'	15°10'	+16°50'	3173	3050		7/8	+ 8.2	I
A 26	Tschierva Vadret	Fm/Fk	26°30'	15°10'	+11°20'	2955	2850–2900	M 3150 Ø 1973	7	+ 6.1/+ 3.2	I
A 27	Roseg Vadret	Fm/Fk	19°40'	11°40'	+ 8°00'	2884	2850	M 3150 Ø 1973	7	+ 2.3	I
A 28	Morteratsch Vadret	Fm/Fk	26°30'	9°20'	+17°10'	2881	2700–2800	M 3010 Ø 1973	7	+ 9.7/+ 4.7	I
A 29	Rhonegletscher	Fm	9°20'	11°50'	− 2°30'	2657	2800–2850	M 2950 Ø 1973	9	− 7.9/−11.5	I
A 30	Triftgletscher	Fm	13°40'	16°00'	− 2°20'	2485	2700–2750	M 2873 Ø 1973	9	−13.0/−16.1	I
A 31	Griesgletscher	Fm	8°40'	8°50'	− 0°10'	2795	2840–2872	I/K/N 2872 1961/62–74/75 A 2840∓50 1962–1975 M 3020 Ø 1973	10	+ 0.6/−11.6	IV
A 32	Oberaletsch-Beichgletscher	Fm/Fk	27°50'	6°30'	+21°20'	2926	2850–2950	M 3170 Ø 1973	11	+ 4.8/− 1.5	II
A 33	Fieschergletscher	Fm	8°50'	9°20'	− 0.30'	2716	2900–2950	M 3193 Ø 1973	12	− 8.8/−11.2	I
A 34	Mittelaletschgl.	Fm	29°00'	12°30'	+16°30'	3034	2850–2950	M 3120 Ø 1973	11	+11.9/+ 5.4	I
A 35	Aletschgletscher	Fm	8°20'	5°00'	+ 3°20'	2689	2850–2950	M 3145 Ø 1973	11	− 6.8/−11.0	I
A 36	Unteraargletscher	Fk	30°30'	5°20'	+25°10'	2804	2650–2700	M 2957 Ø 1973	12	+ 8.6/+ 5.8	II
A 37	Oberaargletscher	Fm/Fk	26°30'	8°20'	+18°10'	2892	2780–2850	M 3007 Ø 1973	12	+ 9.5/+ 3.6	I
A 38	Gauligletscher	Fm	19°00'	10°20'	+ 8°40'	2818	2750–2850	M 2910 Ø 1973	12	+ 5.2/− 2.4	I
A 39	Rosenlauigletscher	Fm	15°30'	25°30'	−10°00'	2725	2650–2750		12	+ 4.5/− 1.5	IV
A 40	Oberer Grindelwaldgl.	Fm	24°30'	22°40'	+ 1°50'	2509	2680–2750		12	− 7.4/−10.5	I
A 41	Unterer Grindelwald-gl./without Ischmeer	Fm/Fk	25°30'	17°20'	+ 8°10'	2551	2600–2650	M 2840 Ø 1973	12	− 1.9/− 3.8	I
A 42	Langgletscher	Fm	23°30'	12°00'	+11°30'	2883	2850–2900	M 3000 Ø 1973	11	+ 1.9/− 1.0	I
A 43	Gamchigletscher	Lk	48°00'	22°40'	+25°20'	2669	2400–2500	M 2520 Ø 1973	11	+19.5/+12.3	I

Tab 1 Geometrical indexes, mathematical indexes and equilibrium line deviation of modern glaciers*)

1	2	3	4	5	6	7	8	9	10	11	12
A 44	Gornergletscher	Fm	19°40'	8°20'	+11°20'	3105	3000–3200	M 3225 ∅ 1973	13/14	+ 4.8/– 4.4	I
A 45	Findelengletscher/ without Adlergl.	Fm	13°10'	8°40'	+ 4°30'	3063	3100–3200	M 3455 ∅ 1973	13/14	– 2.6/– 9.5	I
A 46	Schwarzberggletscher	Fm	30°30'	10°10'	+20°20'	3176	3000–3030	K 3030 1956–1967 M 3170 ∅ 1973	13	+14.1/+12.2	I
A 47	Hohlaubgletscher	Fm	24°30'	16°00'	+ 8°30'	3195	3190	K 3190 1956–1967 M 3160 ∅ 1973	13	+ 0.5	I
A 48	Allalingletscher	Fm	17°20'	12°20'	+ 5°00'	3266	3190	K 3190 1956–1967 M 3293 ∅ 1973	13	+ 4.8	IV
A 49	Gh. del Belvedere	Fk/Lk	45°00'	16°50'	+28°10'	3095	2700–2750		13	+17.2/+13.3	II
A 50	Hohberggletscher	Fm	21°50'	24°30'	– 2°40'	3469	3450	M 3560 ∅ 1973	13	+ 1.2	IV
A 51	Zmuttgletscher	Fm/Fk	37°30'	8°30'	+29°00'	3088	2850–3050	M 3090 ∅ 1973	15	+14.2/+ 2.3	II
A 52	Glacier de Zinal	Fm/Fk	26°40'	10°10'	+16°30'	2956	2880–3200	M 3111 ∅ 1973	16	+ 3.9/– 9.9	II
A 53	Glacier de Ferpècle (Plat. d' Herens)	Fm	15°30'	13°20'	+ 2°10'	2855	3000–3100	M 3200 ∅ 1973	16	– 9.5/–16.0	I
A 54	Glacier du Mont Miné	Fm	13°10'	15°30'	– 2°40'	2802	3000–3100	M 3210 ∅ 1973	16	–12.0/–18.1	I
A 55	Glacier de Moiry	Fm	15°30'	12°50'	+ 2°40'	2961	3000–3050	M 3100 ∅ 1973	16	– 5.1/– 9.3	I
A 56	Haut Glacier d' Arolla	Fm/Fk	29°00'	8°10'	+20°50'	3053	2920–3000	M 3150 ∅ 1973	15	+13.5/+ 5.4	I
A 57	Glacier du M. Collon	Fm	19°40'	21°40'	– 2°00'	2883	2950–3000	M 3100 ∅ 1973	15	– 6.7/–10.2	I
A 58	Glacier de Tsijiore Nouve	Fm/Fk	23°30'	15°30'	+ 8°00'	2974	3000–3100	M 3320 ∅ 1973	15	– 1.9/– 9.4	II
A 59	Glacier d'Otemma	Fm	20°20'	5°50'	+14°30'	3037	3000–3100	M 3126 ∅ 1973	15/17	+ 3.2/– 5.4	I
A 60	Glacier du Giétro	Fm	14°00'	16°00'	– 2°00'	3117	3200	M 3220 ∅ 1973	17	– 7.0	I
A 61	Glacier du Brenay	Fm	17°50'	8°50'	+ 9°00'	3181	3150–3300	M 3293 ∅ 1973	17	+ 2.6/– 9.9	I
A 62	Glacier de Cheilon	Fk	42°10'	9°30'	+32°40'	3183	3000–3100	M 3160 ∅ 1973	17	+18.2/+ 8.3	II
A 63	Glacier de Corbassière	Fm	14°50'	8°40'	+ 6°10'	2970	3000–3150	M 3200 ∅ 1973	17	– 1.9/–11.5	I
A 64	Glacier de Boveire	Fm/Fk	26°30'	16°50'	+ 9°40'	3122	3150–3200	M 3220 ∅ 1973	17	– 2.8/– 7.9	I
A 65	Hohwänggletscher	Fl	16°50'	35°30'	–18°40'	3215	3250	M 3300 ∅ 1973	15	– 4.0	IV

Tab 1 Geometrical indexes, mathematical indexes and equilibrium line deviation of modern glaciers*)

1	2	3	4	5	6	7	8	9	10	11	12
A 66	Glacier de la Dent Blanche	Fl	51°20'	24°30'	+26°50'	3600	3200	M 3240 Ø 1973	16	+26°5	IV
A 67	Glacier du Trient	Fm	20°20'	27°50'	− 7°30'	2610	2800−2900		18/19	−11.7/−17.9	I
A 68	Glacier du Tour	Fm	16°00'	21°50'	− 5°50'	2805	2850−3000		19/20	− 3.3/−14.3	IV
A 69	Gl. d'Argentière	Fm/Fk	35°30'	23°30'	+10°10'	2654	2850−2900		19	− 8.5/−10.7	I
A 70	Mer de Glace	Fm/Fk	12°30'	9°10'	+ 3°20'	2642	2850−3000		19	− 8.4/−14.4	I
A 71	Gl. des Bossons	Fm	21°50'	26°30'	− 4°40'	2864	2900−3000		21	− 1.2/− 4.5	IV
A 72	Gl. du Taconnaz	Fm	30°30'	30°30'	∓ 0°00'	2838	2900−3000		21	− 2.5/− 6.5	IV
A 73	Gl. de Bionnassay	Fm/Fk	26°30'	21°00'	+ 5°30'	2854	2850−3000		21	+ 0.2/− 6.6	I
A 74	Glacier de Miage	Fk	45°00'	16°00'	+29°00'	3156	2850−3000		21	+25.7/+13.1	IV
A 75	Gl. de Tré la Tête	Fm	18°30'	10°40'	+ 7°50'	2857	2850−2950		21	+ 0.4/− 5.4	I
A 76	Gl. de la Lex Blanche	Fm/Fk	30°30'	24°30'	+ 6°00'	2985	3000		21	− 1.0	I
A 77	Glacier du Miage	Fk	32°00'	9°30'	+22°30'	2977	2900		21	+ 3.2	II
A 78	Gl. du Brouillard	Fl	33°30'	27°50'	+ 5°40'	3077	3000−3050		21	+ 3.6/+ 1.3	IV
A 79	Glacier de Frêney	Fl	30°30'	27°50'	+ 2°40'	3203	3050		21	+ 8.7	IV
A 80	Gl. de la Brenva	Fm/Fk	30°30'	19°40'	+10°50'	2821	2850−2900		21	− 1.0/− 2.8	I
A 81	Gl. de Frébouze	Fm/Fk	33°40'	22°40'	+11°00'	3075	2900−2950		19	+16.4/+11.6	IV
A 82	Glacier de Triolet	Fm/Fk	37°30'	17°50'	+19°40'	3054	2850−2900		19	+15.6/+11.8	IV
A 83	Glacier de Saleina	Fm	18°30'	18°30'	∓ 0°00'	2682	2850−3000		20/22	− 8.9/−16.9	I
B 01	Tunsbergdalsbreen	Zf	4°30'	4°00'	+ 0°30'	1150	1382	K/N 1382 1966/67−71/72	23/24	−18.1	I
B 02	Tuftebreen	Zf	6°10'	17°20'	−11°10'	1389	1500−1550		24	− 9.8/−14.2	I
B 03	Nigardsbreen	Zf	6°50'	11°10'	− 4°20'	1110	1487−1570	I/K/N 1487 1962/63−74/75 A 1570∓30 1963−1975	24/25	−24.0/−29.1	I
B 04	Storglaciären	Fm	26°40'	8°40'	+18°00'	1527	1466−1490	I/K/N 1490 1959/60−74/75 I 1466 1959/60−64/65	26	+ 7.4/+ 4.5	I
C 01	Gibsonbreen	Fm	18°30'	7°40'	+10°50'	549	500− 525		27 75/76	+ 8.2/+ 4.0	I
C 02	Ayerbreen	Fm	12°00'	6°40'	+ 5°20'	590	550		27 75/76	+ 6.9	IV
C 03	Scott Turnerbreen	Fm	16°20'	5°10'	+11°10'	573	525− 550		27 75/76	+ 7.4/+ 3.6	I
C 04	Tillbergfonna	Fm	16°50'	6°10'	+10°40'	600	550		27 75/76	+ 8.3	I
C 5	Svendsenbreen	Fm	19°10'	6°30'	+12°40'	683	600− 625		27 75/76	+16.1/+11.3	IV
C 06	Bogerbreen	Fm	16°50'	6°30'	+10°20'	634	575− 600		27 75/76	+ 8.8/+ 5.1	I
C 07	Larsbreen	Fm	8°30'	10°50'	− 2°20'	569	575− 600		27 75/76	− 1.0/− 5.4	I

Tab 1 Geometrical indexes, mathematical indexes and equilibrium line deviation of modern glaciers*)

1	2	3	4	5	6	7	8	9	10	11	12
C 08	Longyearbreen	Fm	25°30'	6°10'	+19°20'	628	550– 575		27 75/76	+11.2/+ 7.6	I
C 09	Tufsbreen	Fm	14°00'	6°30'	+ 7°30'	597	550		27 75/76	+ 7.9	I
C 10	Frostisen/ Skandsdalsbreen	Zf	5°30'	6°40'	– 1°10'	365	420– 450		28/75	– 9.6/–14.9	I
C 11	Frostisen/ Studentdalenbreen	Zf	12°50'	11°20'	+ 1°30'	428	420– 450		28/75	+ 1.8/– 4.8	I
C 12	Jotunfonna/middle Tordalenbreen	Zf	9°10'	11°20'	– 2°10'	472	520		28/75	–10.8	I
C 13	Jotunfonna/ Elicher Tordalenbr.	Zf	6°30'	9°30'	– 3°00'	478	520		28/75	– 9.0	I
C 14	Manchester/ Southhamptonbreen	Fm	14°50'	4°00'	+10°50'	506	400		29/75	+18.9	IV
C 15	Hörbyebreen	Fs/Fm	12°20'	3°10'	+ 9°10'	483	450– 470		29/75	+ 4.3/+ 1.7	IV
C 16	Bertilbreen	Fm	19°00'	5°10'	+13°50'	498	460– 500		29/75	+ 5.1/– 0.3	I
D 01	Qaqugdluit/E-outlet (70°6'N/51°34'W)	Zf	6° 00'	18°30'	–12°30'	713	900		30 77/78	–16.3	I
D 02	Qaqugdluit/E-outlet (70°5'N/51°34'W)	Zf	5°50'	13°10'	– 7°20'	692	850– 900		30 77/78	–14.3/–18.9	I
D 03	Qaqugdluit/E-outlet (70°8'N/51°34'W)	Zf	17°50'	8°00'	+ 9°50'	873	850		30 77/78	+ 2.9	IV
D 04	Qaqugdluit/NE-outlet (70°10'N/51°38'W)	Zf	10°20'	4°10'	+ 6°10'	929	850		30 77/78	+14.2	IV
D 05	Qaqugdluit/NNW-outlet (70°10'N/51°49'W)	Zf	11°20'	6°10'	+ 5°10'	949	850– 875		30 77/78	+14.0/+10.6	IV
D 06	Qaqugdluit/W-outlet (70°7'N/51°54'W)	Zf	17°20'	11°30'	+ 5°50'	869	875		30 77/78	– 0.8	I
D 07	Qaqugdluit/S-outlet (70°5'N/51°47'W)	Zf	7°50'	6°20'	+ 1°30'	898	900– 950		30 77/78	– 0.3/– 8.7	I
D 08	Qaqugdluit/S-outlet (70°4'N/51°46'W)	Zf	6°00'	14°20'	– 8°20'	725	875– 900		30 77/78	–15.8/18.4	I
D 09	Nûgssuaq/Sermerssuaq (70°20'N/51°41'W)	Zf	7°40'	8°20'	– 0°40'	988	1000–1100		31 77/78	– 1.3/–12.5	I
D 10	Nûgssuaq/Sermerssuaq (70°21'N/51°52'W)	Zf	9°10'	8°30'	+ 0°40'	986	1000–1100		31 77/78	– 1.4/–11.7	I
D 11	Nûgssuaq/Sermerssuaq (70°22'N/52°0'W)	Zf	10°50'	5°50'	+ 5°00'	1058	1050–1100		31 77/78	+ 0.7/– 3.8	I
D 12	Nûgssuaq/Sermerssuaq (70°22'N/52°7'W)	Zf	10°10'	7°20'	+ 2°50'	1114	1150–1200		31 77/78	– 3.5/– 8.4	I
D 13	Nûgssuaq/Sermerssuaq (70°23'N/52°12'W)	Zf	15°10'	10°10'	+ 5°00'	1170	1200		31 77/78	– 3.2	I
D 14	Nûgssuaq/Sermerssuaq (70°31'N/51°56'W)	Zf	8°30'	5°10'	+ 3°20'	845	1100		31/32 77/78	–15.8	I
D 15	Nûgssuaq/Sermerssuaq (70°29'N/51°54'W)	Zf	10°10'	6°40'	+ 3°30'	945	1100–1150		31 77/78	–11.2/–14.7	I
D 16	Nûgssuaq/Sermerssuaq (70°35'N/52°20'W)	Zf	13°20'	4°40'	+ 8°40'	1212	1200–1250		33/34 77/78	+ 0.9/– 2.8	I

Tab 1 Geometrical indexes, mathematical indexes and equilibrium line deviation of modern glaciers*)

1	2	3	4	5	6	7	8	9	10	11	12
D 17	Nûgssuaq/Sermerssuaq (70°27'N/52°28'W)	Zf	11°30'	4°40'	+ 6°50'	1083	1100		31/34 77/78	− 1.2	I
D 18	Nûgssuaq/Sermerssuaq (70°32'N/52°4'W)	Zf	15°10'	6°40'	+8°30'	1078	1100−1150		32 77/78	− 1.6/− 5.3	I
D 19	Nûgssuaq/Sermerssuaq (70°34'N/52°5'W)	Zf	14°00'	7°40'	+ 6°20'	1050	1100−1200		32 77/78	− 2.8/− 8.3	I
E 01	Blue Glacier (47°50'N/123°45'W)	Fm	20°20'	11°10'	+ 9°10'	1798	1719−1860	I/K 1719 1963/64−66/67 A 1860∓90 1964−1968	35	+ 7.6/− 5.9	I
E 02	Peyto Glacier	Fm	13°10'	7°30'	+ 5°40'	2589	2630−2666	A 2630∓30 1965−1975 K/N 2666 1965−1975	36	− 4.5/− 8.4	I
E 03	Lemon Creek Glacier (58°50'N/134°20'W)	Fm	5°30'	11°50'	− 6°20'	950	1075		37	−13.9	I
E 04	Worthington Glacier (61°10'N/145°40'W)	Fm	10°50'	10°30'	+ 0°20'	1248	1310		38	− 5.3	I
E 05	Bear Lake Glacier (60°10'N/149°20'W)	Fm	14°20'	8°40'	+ 5°40'	942	925− 950		39	+ 1.5/− 0.7	I
E 06	McCall Glacier (69°20'N/143°45'W)	Fm	11°10'	7°30'	+ 3°40'	1937	1925−2068	N 2068 1968/69−71/72	40	+ 1.0/−10.7	I
E 07	Muldrow Glacier	Fs	20°20'	2°20'	+18°00'	2489	2134−2439		41/42	+11.3/+ 1.6	I
E 08	Peters Glacier	Fs	24°30'	5°00'	+19°30'	2560	2195−2300		43/44	+11.3/+ 8.1	I
E 09	Peters Dome-N-Gl.	Fk	33°40'	8°10'	+25°30'	1995	1982−2104		41	+ 0.8/− 6.8	II
E 10	Ruth Glacier	Fs	10°30'	2°00'	+ 8°30'	1907	1650		45−47	+ 7.7	I
E 11	Kahiltna Glacier	Fs	14°20'	2°10'	+12°10'	2179	1677−1829		41/44 48−51	+13.0/+ 9.0	I
E 12	Tokositna Glacier	Fs	16°50'	2°30'	+14°20'	1743	1500−1615		46−48	+ 8.3/+ 4.1	II
E 13	Yentna/Lacuna Gl.	Fs	12°30'	2°00'	+10°30'	1646	1650−1829		48 52/53	− 0.1/− 6.5	II
E 14	Dall Glacier	Fs	7°50'	3°00'	+ 4°50'	1304	1400−1550		52−55	− 4.3/−11.1	I
E 15	Chedotlothna Gl.	Fs/Fk	21°00'	2°30'	+18°30'	1777	1550−1700		52/55	+12.3/+ 4.2	I
E 16	Surprise Glacier	Fs	6°40'	4°10'	+ 2°30'	1371	1372−1524		54	∓ 0.0/−12.6	I
E 17	Glacier (62°57'N/151°50'W)	Fk	33°40'	5°50'	+27°50'	1897	1677−1829		52	+14.6/+ 4.5	II
E 18	Herron Glacier	Fs/Fk	32°00'	4°50'	+27°10'	2469	2000		48/52 56	+15.4	II
E 19	Foraker Glacier	Fk	35°30'	4°20'	+31°10'	2510	1982−2287		44/56 48	+16.2/+ 6.9	II
E 20	Straightaway Gl.	Fk	20°20'	4°00'	+16°20'	2297	2195−2287		44	+ 3.9/+ 0.4	II
E 21	Buckskin Glacier	Fs	21°00'	3°10'	+17°50'	1539	1350−1460		43/47 57	+ 8.9/+ 3.7	I
E 22	Kanikula Glacier	Fs/Fk	21°50'	4°30'	+17°20'	1423	1311−1524		46/49 48	+ 5.2/− 4.7	II
E 23	Malaspina Glacier	Fs	33°40'	1°20'	+32°40'	2108	900−1000	O 1000	58/59	+28.7/+26.3	IV

Tab 1 Geometrical indexes, mathematical indexes and equilibrium line deviation of modern glaciers*)

1	2	3	4	5	6	7	8	9	10	11	12
E 24	Bering Glacier	Fs	2°30'	0°50'	+ 1°40'	1480	900–1000	O/F 1000 · 1949	58/60	+21.6/+17.9	IV
E 25	Kaskawulsh Glacier	Fs	2°50'	1°40'	+ 1°10'	1973	2150–2300		58	– 7.3/–13.5	I
F 01	Ndo. Soirococha NW-Gl.	Fl	37°40'	26°30'	+11°10'	4751	4700–4720		61	+ 7.7/+ 4.7	I
F 02	5455 m-peak-N-Gl.	Fl	37°40'	33°40'	+ 4°00'	4855	4800–4850		61	+ 5.9/+ 0.5	IV
F 03	5435 m-peak-N-Gl.	Fl	37°40'	35°30'	+ 2°10'	5009	4850		61	+19.0	IV
F 04	5540 m-peak-N-Gl.	Fl	48°00'	32°00'	+16°00'	4953	4850		61	+ 9.7	IV
F 05	Panta o Chacha-cumayoc-N-Gl.	Fl	45°00'	32°00'	+13°00'	4970	4850		61	+13.3	IV
G 01	Glacier 5Y813B 8	Fk	35°30'	10°10'	+25°20'	4259	3950–4000	P	62	+17.6/+14.7	I
G 02	Glacier 5Y813B 11	Fk/Lk	55°00'	11°10'	+43°50'	4393	4000–4050	P	62	+29.2/+25.5	I
G 03	Glacier 5Y813B 17	Fk/Lk	55°00'	15°30'	+39°30'	4370	4000–4050	P	62	+26.4/+22.9	I
G 04	Glacier 5Y813C 10	Fk	55°00'	7°10'	+47°50'	4134	3750–3800	P	62	+26.2/+22.7	I
G 05	Glacier 5Y725B 8	Fk/Lk	45°00'	16°00'	+29°00'	4157	3800–3850	P	62	+21.1/+18.1	I
G 06	Glacier 5Y725B 10	Fk	39°30'	8°10'	+31°20'	4202	3850–3900	P	62	+20.3/+14.5	I
G 07	Glacier 5Y725E 10	Fk/Lk	48°00'	9°20'	+38°40'	4388	3950–3990	P	62	+26.7/+24.3	I
H 01	Fedtschenko Gl.	Fs	4°40'	2°10'	+ 2°30'	4385	4600–4750	B 4600	63	– 7.3/–12.3	I
H 02	Notgemeinschaftsgl.	Fs	8°10'	3°10'	+ 5°00'	4794	4800–4900	B 4800	63	– 0.2/– 4.4	I
H 03	Tanimas 2 Gl.	Fm	15°10'	8°10'	+ 7°00'	4945	4800	B	63	+ 6.5	I
H 04	Tanimas 3 Gl.	Fm	22°40'	5°40'	+17°00'	4980	4700–4800	B	63	+14.9/+ 9.6	I
I 01	Dunde-SE-outlet	Zf	11°30'	14°50'	– 3°20'	5003	5060		64	–12.8	I
I 02	Dunde-SSW-outlet	Zf	10°50'	10°50'	± 0°00'	4975	5100		64	–19.8	I
I 03	Dunde-middle SSW-outlet	Zf	9°20'	11°30'	– 2°10'	5024	5100		64	–15.5	I
I 04	Dunde-SSW-outlet	Zf	10°30'	11°50'	– 1°20'	5084	5150–5200		64	–12.2/–21.6	I
I 05	Dunde-N-outlet	Zf	18°20'	11°10'	+ 7°10'	5086	5080		64	+ 1.1	I
I 06	Dunde-N-outlet/ 2nd from W	Zf	17°20'	7°00'	+10°20'	5046	5050–5080		64	– 0.7/– 6.2	I
I 07	Dunde-N-outlet/ 2nd from E	Zf	7°40'	6°20'	+ 1°20'	4985	5050		64	–10.7	I
I 08	Dunde-EN-outlet	Zf	5°40'	8°40'	– 3°00'	4935	5050		64	–16.2	I
K 01	Halun Glacier	Fm/Fk	27°50'	8°40'	+19°10'	5342	5000–5050		65	+20.9/+17.9	I
K 02	Ha Lang Glacier	Fm/Fk	21°50'	6°20'	+15°30'	5220	5000–5050		65	+16.4/+12.7	I
L 01	Batura Glacier	Fk	26°40'	3°10'	+23°30'	4669	4800–5100	R 5000	66	– 3.1/–10.2	II
L 02	Minapin Glacier	Fk	32°00'	9°50'	+22°10'	4274	4100–4200		67	+ 4.5/+ 1.9	II
L 03	Pisan Glacier	Lk	48°00'	16°50'	+31°10'	4850	4200		67	+13.3	III
M 01	Bazhin Gl.	Lk	51°40'	12°50'	+38°50'	5354	4600–4900	D 4700–4800	68	+17.9/+10.8	III
M 02	Shaigiri-Gl.	Fk/Lk	48°00'	17°20'	+30°40'	5404	4900	D	68	+14.0	III

Tab 1 Geometrical indexes, mathematical indexes and equilibrium line deviation of modern glaciers*)

1	2	3	4	5	6	7	8	9	10	11	12
M 03	Hanging Glacier	Lk/Fl	51°40'	27°50'	+23°50'	5716	4900	D	68	+19.4	III
M 04	Chhungphar/ Chongra-Gl.	Lk	39°50'	12°20'	+27°30'	4720	4600–4900	D	68	+ 3.2/– 4.9	II
M 05	Sachen Gl.	Lk	42°10'	9°30'	+32°40'	4706	4600–4700	D	68	+ 3.9/+ 0.2	II
M 06	Rakhiot-Gl.	Fk	32°00'	9°30'	+22°30'	5065	4750–4800	D	68	+ 8.3/+ 7.0	I
M 07	Dhaulagiri-S-Gl.	Fk/Lk	32°00'	18°30'	+13°30'	5602	5500–5600		69	+ 3.2/+ 0.06	III
M 08	Dhaulagiri-E-Gl.	Fk/Lk	27°50'	25°30'	+ 2°20'	5194	5500–5600		69	– 8.8/–11.6	I
M 09	Dhaulagiri-N-Gl.	Fk/Lk	25°30'	10°00'	+15°30'	5539	5500–5600		69	+ 1.1/– 1.7	III
M 10	Roc Noir-NNE-Gl.	Fk	37°30'	14°10'	+23°20'	5659	5500–5550		69	+ 5.1/+ 3.5	III
M 11	Lower Barun Glacier	Fm/Fk	13°10'	7°20'	+ 5°50'	5623	6000–6050		70	–17.7/–20.1	II
M 12	Khumbu Glacier	Fk	39°50'	7°30'	+32°20'	6432	5600–5720	L 5720	70/71	+27.2/+23.2	III
M 13	Barun Glacier	Fk	30°30'	4°30'	+26°00'	5841	5800–6000		70	+ 2.2/– 8.6	II
M 14	Lhotse Glacier	Lk	59°00'	12°20'	+46°40'	6585	5600–5750	L 5750	70/71	+29.6/+25.1	III
M 15	Lhotse Shar/Imia Gl.	Lk	45°00'	7°50'	+37°10'	6154	5700–5730	L 5730	70/71	+20.9/+19.5	III
M 16	Amai Dablang Gl.	Lk	59°00'	10°10'	+48°50'	5646	5300–5400	L 5400	70/71	+19.5/+13.9	II
M 17	Chhukhung Glacier NE-component	Fl	39°50'	19°00'	+20°50'	5615	5450–5570	L 5570	70/71	+13.9/+ 3.8	IV
M 18	Hunku Nup Glacier	Fk	39°50'	7°10'	+32°40'	5785	5560–5600		70	+25.3/+20.8	I
M 19	Hunku Glacier	Fk	51°30'	10°10'	+41°20'	6045	5800		70	+14.5	II
M 20	Makalu-W-Glacier (with Chago Gl.)	Lk	51°40'	14°00'	+37°40'	6619	5900–6100		70	+25.0/+18.0	III
M 21	Lhotse Nup Gl.	Lk	59°00'	15°10'	+43°50'	6360	5600–5700	L 5700	70/71	+27.1/+23.6	III
M 22	Nuptse Glacier	Lk	59°00'	11°30'	+47°30'	6360	5600–5700	L 5700	70/71	+27.1/+23.6	III
M 23	Hunku Shar Gl.	Fk/Lk	33°40'	7°10'	+26°30'	5965	5850–5900		70	+ 9.3/+ 5.3	II
M 24	Changri Shar Gl.	Lk	55°00'	9°30'	+45°30'	5985	5700–5750	L 5700	70/71	+17.7/+14.6	II
M 25	Changri Nup Gl.	Lk	48°00'	6°10'	+41°50'	5833	5600–5800	L 5620	70/71	+17.8/+ 2.5	II
M 26	Gyubanare Glacier	Lk	45°00'	5°10'	+39°50'	5868	5650–5800	L 5670	70	+12.0/+ 3.7	II
M 27	Lungsampa/Ngozumpa Glacier	Fk	29°00'	4°20'	+24°40'	6058	5580–5650	L 5580	70	+17.4/+14.8	III
M 28	Sumna Glacier	Lk	39°50'	7°20'	+32°30'	6060	5650–5750	L 5750	70	+17.3/+13.1	III
M 29	W-Col-W-Glacier (S of Hunku Gl.)	Fk	48°00'	12°30'	+35°30'	5980	5750–5800		70	+25.0/+19.6	I
M 30	Nangpa Lunag Gl.	Lk	45°00'	4°20'	+40°40'	5704	5600–5800	L 5800	70	+ 5.3/– 4.9	II
M 31	Pangbug Glacier	Lk	55°00'	5°50'	+49°10'	5789	5500–5600	L 5600	70	+19.3/+12.6	II
M 32	Dingjung Glacier	Lk	51°20'	8°50'	+42°30'	5666	5400	L 5400	70	+16.3	II
M 33	Langmoche Glacier	Lk	48°00'	19°40'	+28°20'	5572	5300–5500	L 5500	70	+11.6/+ 3.1	II
M 34	Kangshung Glacier	Lk	39°50'	5°30'	+34°20'	6127	5500–5600		70/72	+20.3/+17.0	III
M 35	Tuo Glacier	Lk	59°00'	18°30'	+40°30'	5653	5300–5400	L 5300	70/71	+20.2/+14.5	II
M 36	Lobuche Glacier	Fk	29°00'	14°20'	+14°40'	5566	5500–5570	L 5570	70	+ 5.8/– 0.4	II

Tab 1 Geometrical indexes, mathematical indexes and equilibrium line deviation of modern glaciers*)

1	2	3	4	5	6	7	8	9	10	11	12
M 37	SE-Tsola Gl.	Lk	63°40'	18°30'	+45°10'	5492	5300–5450	L 5450	70	+10.3/+ 2.3	II
M 38	W-Rongbu Gl.	Fk	39°50'	3°30'	+36°20'	6206	5860–6200	G 5900–6100	72	+16.4/+ 5.0	III
M 39	E-Rongbu Gl.	Fk	22°40'	5°00'	+17°40'	6318	6200		72	+ 7.2	III
M 40	Rongtö Glacier (Gyachung-Kang-NE-Gl.)	Fk	37°30'	6°10'	+31°20'	6141	6100		72	+ 2.8	II
M 41	Gyachung Kang Gl.	Fk	48°00'	5°20'	+42°40'	6414	6000–6050		72	+17.8/+15.6	III
M 42	Gyabrag Glacier (Nangpa La-N-Gl.)	Fk	26°40'	4°30'	+22°10'	6064	5850–6100	G 6100	70/72	+ 9.9/− 1.7	III
M 43	Drolambao Glacier (Trakarding tongue)	Fk/Lk	24°30'	6°00'	+18°30'	5509	5400–5650		73	+ 5.6/− 7.2	II
M 44	Ripimo Shar Glacier	Fk	35°30'	6°50'	+28°40'	5506	5450		73	+ 3.0	II
M 45	Dropga Nagtsang Gl.	Fk	32°00'	6°00'	+26°00'	5722	5500–5650		73	+14.6/+ 4.7	II
M 46	Zemu Glacier	Fk	30°30'	4°10'	+26°20'	5617	5400	C 5400	74	+ 7.0	III

***) Table Key**

(1) Regional association and notation
A = Alps, B = Scandinavia, C = W Spitsbergen, D = W Greenland, E = North America/Alaska, F = South America, G = Tian Shan, H = Alai Pamir, I = Kuen Lun, K = Anyemaquen, L = Karakoram, M = High Himalayas
(2) Name of the glacier and/or coordinates of the terminus
(3) Glacier type according to the terminology of Schneider (1962)
(Zf) = central firn cap, (Fk) = firn caldron type, (Fm) = firn basin type, (Lk) = avalanche caldron type, (Fs) = firn stream type, (Fl) = flank glaciation/wall glaciation
(4) Angle α (°)
(5) Angle δ (°)
(6) Geometrical index (I_g) = $\alpha - \delta$
(7) Mathematical index (I_m)
(8) Equilibrium line altitude
(9) Literature sources for equilibrium line values (A–R)**)
(10) Maps (1)–(74)***)
(11) Maximum and minimum amounts of the factor of equilibrium line deviation: FED = $\frac{(I_m - ELA) \times 100}{\text{vertical distance}}$
(12) Group affiliation (I/II/III)

****) References for equilibrium line values (Tab 1, col. 9)**

(A) Braithwaite, R. J.; Müller, F. (1980)
(B) Finsterwalder, R. (1932)
(C) Finsterwalder, R. (1933)
(D) Finsterwalder, R. (1938)
(E) Gross, G.; Kerschner, H.; Patzelt, G. (1977)
(F) Hermes, K. (1965)
(G) Heuberger, H. (1956)
(H) Jiresch, E. (1982)
(I) Kasser, P. (1967)
(K) Kasser, P. (1973)
(L) Müller, F. (1970)
(M) Müller, F.; Caflisch, T.; Müller, G. (1976)
(N) Müller, F. (1977)
(O) Sharp, R. P. (1951)
(P) Wang Yinsheng; Qiu Jiaqi (1983)
(R) Zhang Xiangsong; Chen Jinming; Xie Zichu; Zhang Jinhua (1980)

*****) Maps (Tab 1, Col. 10)**

(1) Karte d. Ötztaler Alpen/Blatt Weisskugel-Wildspitze; ÖAV 1951; Feldarbeiten 1942/43–1950.
(2) Karte d. Ötztaler Alpen/Blatt Gurgl, DÖAV 1949; Feldarbeiten 1938/1943 u. 1948.
(3) Vernagtferner 1:10000, Blatt 3 (1938–1969), Kom. f. Glaz. d. Bayerischen Akad. d. Wiss., München 1972. – In: Kasser, P., Fluctuations of Glaciers 1965–1970, 1973.
(4) Luftbildkarte "Großvenediger" 1:10000. Pillewizer, W. (ed.): Glaziologie und Kartographie. W. Pillewizer Festschrift, Geowiss. Mitt. 21, Wien 1982.
(5) Landeskarte der Schweiz (LKS) 1:25000 / Blatt 1198; Gletscherstand 1956.
(6) LKS 1:25000 / Blatt 1178; Gletscherstand 1959.
(7) LKS 1:50000 / Blatt 268; Aufnahme 1934–1948
(8) LKS 1:50000 / Blatt 269; Aufnahme 1965
(9) LKS 1:50000 / Blatt 255; Gesamtnachführung 1960, Nachträge 1965
(10) LKS 1:50000 / Blatt 265; Gletscherstand 1959
(11) LKS 1:50000 / Blatt 264; Gletscherstand: Gletscherzunge 1970 übrige Gletscher 1957–70
(12) LKS 1:5000 / Blatt 5004; Gesamtnachführung 1969/71, Einzelnachträge 1971/74
(13) LKS 1:50000 / Blatt 284; Gesamtnachführung 1968
(14) LKS 1:25000 / Blatt 1348; Gletscherstand 1963
(15) LKS 1:25000 / Blatt 1347; Gletscherstand 1967
(16) LKS 1:50000 / Blatt 283; Gesamtnachführung 1961, 1968
(17) LKS 1:25000 / Blatt 1346; Gletscherstand 1964
(18) LKS 1:50000 / Blatt 282; Ausgabe 1954
(19) Carte Touristique 1:25000, Massif du mont blanc (1); Institut Géographique National 1975.
(20) LKS 1:25000 / Blatt 1344; Gletscherstand 1960
(21) Carte Touristique 1:25000, Massif du mont blanc (2); Institut Géographique National, Paris 1975.
(22) LKS 1:25000 / Blatt 1345; Gletscherstand 1961
(23) Norge Norway 1:50000 / Blatt 1318 II; Gletscherstand 1966
(24) Norge Norway 1:50000 / Blatt 1418 III; Gletscherstand 1966
(25) Norge Norway 1:50000 / Blatt 1418 IV; Gletscherstand 1966
(26) Topografisk Karta över Sverige 1:100000 / Blatt 29 I: Kebnekaise; Gletscherstand 1961
(27) Svalbard 1:50000 / Blatt E 9; Norsk Polarinstitutt, Oslo.
(28) Svalbard 1:100000 / Blatt C 8 / Billefjorden; Norsk Polarinstitutt, Oslo 1970/71
(29) Svalbard 1:100000 / Blatt C 7 / Dicksonfjorden; Norsk Polarinstitutt, Oslo 1972

(30) Danmark / Grönland 1:50000 / Blatt 70 V. 20; Geodetic Inst. Copenhagen 1958
(31) Danmark / Grönland 1:50000 / Blatt 70 V.2K
(32) Danmark / Grönland 1:250000 / Blatt 70 V.2 / Umanak; Stand 1948/1953
(33) Danmark / Grönland 1:50000 / Blatt 70 V.2E
(34) Danmark / Grönland 1:50000 / Blatt 70 V.2J
(35) "Nine Glacier Maps" 1:10000; Am. Geogr. Soc., Spec. Publ. no. 34 (1960); Sheet no. 2; Gletscherstand 1957
(36) "Peyto Glacier" 1:10000; Part of 82 N 10/E; Inland Water Directorate, 1975; Gletscherstand August 1966. In: Müller, F., Fluctuations of Glaciers 1970–1975, 1977.
(37) "Nine Glacier Maps" 1:10000; Am. Geogr. Soc., Sec. Publ. no. 34 (1960); Sheet no. 1; Gletscherstand September 18, 1957
(38) "Nine Glacier Maps" (. . .); Sheet no. 5; Gletscherstand May 17, 1957
(39) "Nine Glacier Maps" (. . .); Sheet no. 7; Gletscherstand July 8, 1957
(40) "Nine Glacier Maps" (. . .); Sheet no. 9; Gletscherstand Aug. 26, 1958
(41) Mount McKinley, Alaska 1:50000, B. Washburn, Gletscherstand 1951. In: Schweiz. Stiftg. f. alpine Forschung (ed.) Berge der Welt 1960/61.
(42) Alaska Topographic Series (ATS) 1:250000 / Mt. McKinley; Gletscherstand 1952–1958
(43) ATS 1:63360 Mt McKinley (A-2); Stand 1952
(44) ATS 1:63360 Mt McKinley (A-3); Stand 1952
(45) ATS 1:63360 Talkeetna (C-1); Stand 1951+53
(46) ATS 1:63360 Talkeetna (C-2); Stand 1953–54
(47) ATS 1:63360 Talkeetna (D-2); Stand 1952
(48) ATS 1:63360 Talkeetna (D-3); Stand 1952
(49) ATS 1:63360 Talkeetna (C-3); Stand 1951–54
(50) ATS 1:63360 Talkeetna (B-3); Stand 1951–54
(51) ATS 1:250000 / Talkeetna; Gletscherstand 1954–58
(52) ATS 1:63360 Talkeetna (D-4); Stand 1952
(53) ATS 1:63360 Talkeetna (C-4); Stand 1952/53
(54) ATS 1:63360 Talkeetna (C-5); Stand 1952+57
(55) ATS 1:63360 Talkeetna (D-5); Stand 1952
(56) ATS 1:63360 Mt McKinley (A-4); Stand 1952
(57) ATS 1:63360 Talkeetna (D-1); Stand 1951–54
(58) ATS 1:250000 / Mt. St. Elias; Stand 1961
(59) ATS 1:250000 / Yakutat; Stand 1948–59 und 1963
(60) ATS 1:250000 / Bering Glacier; Stand 1957
(61) Cordillera Vilcabamba, Perú / Blatt Panta 1:25000. E. Spiess; In: Schweiz. Stiftg. f. Alpine Forschung (ed.), Berge der Welt, Bd. 15, Zürich 1965.
(62) Glacial Topographic Map of Mt. Bogda Region, 1:50000. Journ. of Glaciology and Cryopedology 5, 3 (1983).
(63) Fedtschenko Tanimasgebiet / Blatt Süd und Nord / 1:50000, Finsterwalder, R.; Biersack, H.; Notgemeinschaft d. Dt. Wiss., 1930.
(64) The Map of Dunde Glacier, 1:50000, Academia Sinica, 1982.
(65) Climatic Geomorphological Map of Anyemaqen Region, 1:100000, by Wang Jin-Tai and Gu pei; Gletscherstand 1981
(66) The Map of Batura Glacier, 1:60000; compiled by the Inst. of Glaciol. and Cryopedol. and Desert Research, Academia Sinica, Lanchow 1978; Prof. Papers on the Batura Glacier, Karakoram Mountains 1980.
(67) Minapin (Rakaposhi Range) NW-Karakorum, 1:50000; Stand 1954, Schneider, H.-J., Berlin 1967.
(68) Karte der Nanga Parbat-Gruppe, 1:50000; Deutsche Himalaya Expedition 1934. In: Finsterwalder, R., et al. (eds.). Die geodätischen, gletscherkundlichen u. geographischen Ergebnisse d. Dt. Himalaya Exp. 1934 zum Nanga Parbat. Berlin 1938.
(69) Geomorphologische Karte des Dhaulagiri- und Annapurna-Himalaya 1:85000 von M. Kuhle; Grundlage: One Inch (1:63360) Topographic Map, Survey of India, Aufnahme 1958–1967; Kuhle, M.: Der Dhaulagiri- und Annapurna-Himalaya. Z. F. Geomorphologie, Suppl. Bd. 41, Stuttgart/Berlin 1982.
(70) Khumbu Himal (Nepal) 1:50000, E. Schneider et al., Aufnahme 1955–1963. Hellmich, W. (ed.) Forschungsunternehmen Nepal Himalaya.
(71) Chomolongma-Mount Everest 1:25000, E. Schneider et al., Stand 1955. (ed.) by Dt. Alpenverein u. Österr. Alpenverein and Dt. Forschungsgemeinschaft, 1957.
(72) Qomolangma Feng Region 1:50000, "Mount Jolmo Lungma Scientific Expedition 1966–1968", Academia Sinica, China.
(73) Rolwaling Himal (Gaurisankar), Nepal, 1:50000, E. Schneider et al., Aufnahme 1960–1968. Hellmich, W. (ed.) Forschungsunternehmen Nepal Himalaya.
(74) Karte des Zemu-Gletschers (Sikkim-Himalaya) 1:33333, Finsterwalder, R.; Wien, K.. In: Bauer, P. Um den Kantsch. Der zweite deutsche Angriff auf den Kangchendzönga 1931. München 1933.

Images

(75) Svalbard, Serie 1148 / S60, 1:50000, vom 7./9. Juli 1960; Norsk Polarinstitutt, Oslo.
(76) Svalbard, Serie 1248 / S61, 1:40000, vom 23.–25. 8. 1961, Norsk Polarinstitutt, Oslo.
(77) Grönland, Serie 520, 15. 7. 1948; Geodetic Institute, Denmark.
(78) Grönland, Serie USN VJ-62 DET. "A" 77/148, 5. 6. 1953, "A" 98/145, 24. 6. 1953; Geodetic Institute, Denmark.

Firn and ice formation occur comparatively slowly here and dependent on the growing overburden pressure of accumulating snow masses. Particularly the long-term accumulation of snow at high altitudes is usually checked by lacking depositional surfaces and intensive wind drifting – the empirical upper boundary of glaciation is achieved here (Fig 6, 7; Kuhle 1986b). Therefore, in catchment areas over 7000 m an accumulation capability which is too low relative to the average summit elevation and consequently disproportionally short glacier tongues are to be expected. This would have to be expressed in an increase in equilibrium line deviation through the resulting increase in I_m. In the consistent classification of catchment areas over 7000 m undertaken here it is however problematic that mass balances are not always negative but also positive, as in some cases on leeward slopes. Moreover, there is a regional and meridian-parallel variation in the upper boundary of glacier-formation, corresponding to that of the recrystallization zone (cf. Shumskii 1964, Fig 122). A general limitation to catchment areas over 7000 m, as in the case presented here, is only preliminary. This is acceptable here because all examples originate from the Himalayas and other glaciations which partly extend into the recrystallisation zone: for example Antarctica and the inland ice of central Greenland (Shumskii 1964, 408) are not used in this comparison. In summary, it is maintained that the specified, influencing distortional effects do show a tendency of increasing or decreasing the equilibrium line deviation, but only contingently allow conclusions on the absolute amounts. Other distortional effects which may affect the equilibrium line deviations like the regional variability of activity indexes (cf. Andrews 1975, 21–30) are conceivable, but are too complex and uncalculable especially regarding subrecent glaciations, and thus it is not possible to consider them. It is also to be assumed

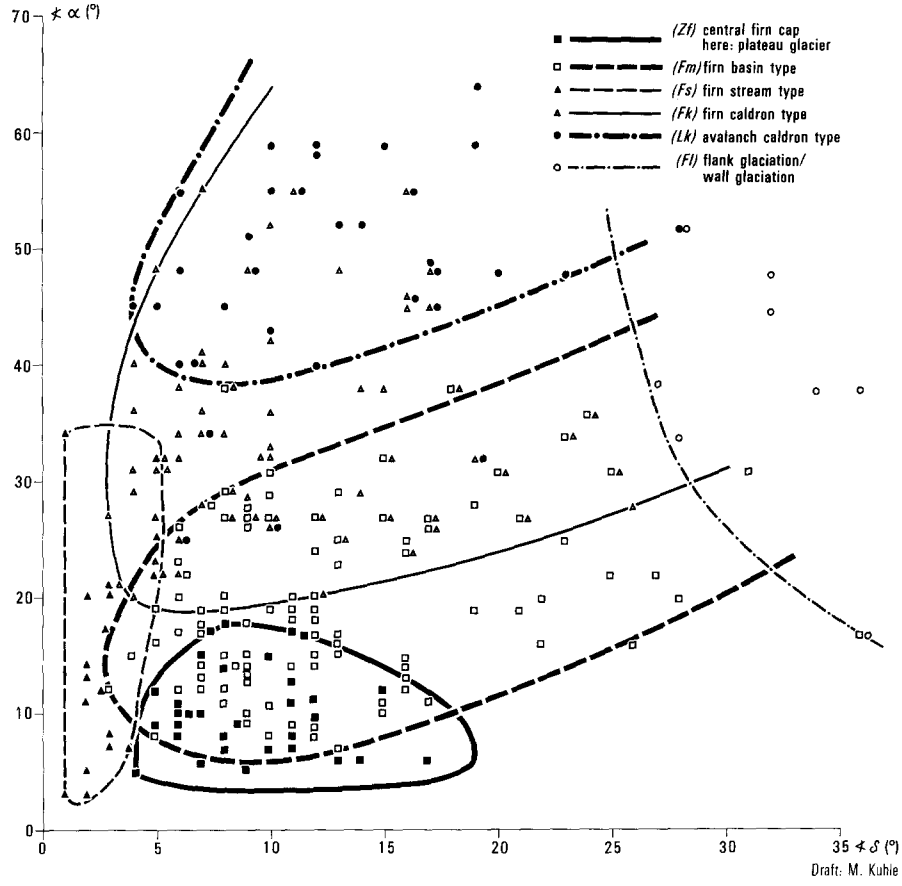

Fig 4
Glacier-typological scatter diagram based on the angles α and δ (Tab 1, col. 4+5)

that the glaciers chosen for comparison are in various stages of mass balance (negative, equalized, positive) with which a variation in the deviation factors must also be related. Thereby, it should be emphasized that concerning the amounts of equilibrium line deviation only integral values can be obtained (i.e. random variables) whose empirical dependency on the angle differences can only be expressed through a large number of glaciers with a more or less wide range of variation and not through a strictly functional correlation of both factors using individual cases. This range of variation in the equilibrium line deviation has advantages in reconstructing subrecent glaciations. Since the climatic and other parameters are never to be deduced a priori with the required exactness for using them in ELA calculation, the method of reconstruction must reflect the disregard of these parameters in the form of a corresponding inaccuracy. A greater accuracy can only be acquired with complemental studies, such as pollen analysis. Methods with which a calculation of a subrecent or recent ELA is designed for a definitive value from the outset can obtain this "accuracy" only through an averaging method with which the variations through marginal influences are omitted (see discussion of AAR method above). This eliminates the possibility for a subsequent specification of the values corresponding, for instance, to the regional climatic or topographic relationships, as they can be at least tendentiously evaluated in individual cases.

Correlation of Equilibrium Line Deviation and Geometrical Index

Concurring with the previous considerations the 223 glaciers studied were divided into 4 groups (Tab 1, col. 12):

Group I (n=130): Glaciers with ablation zones which are canalized by valley slopes, free of debris or have a debris cover of less than 25%, and have average summit heights less than 7000 m.

Group II (n= 39): Glaciers whose ablation zones are more than 25% covered with debris and whose average summit heights are less than 7000 m.

Group III (n= 21): Glaciers whose average summit heights are over 7000 m (all of the glaciers belonging to this group incidentally have ablation zones with debris cover over 25%).

Group IV (n= 33): Glaciers with uncanalized, outflowing, calving or interrupted ablation zones covered up to 25%

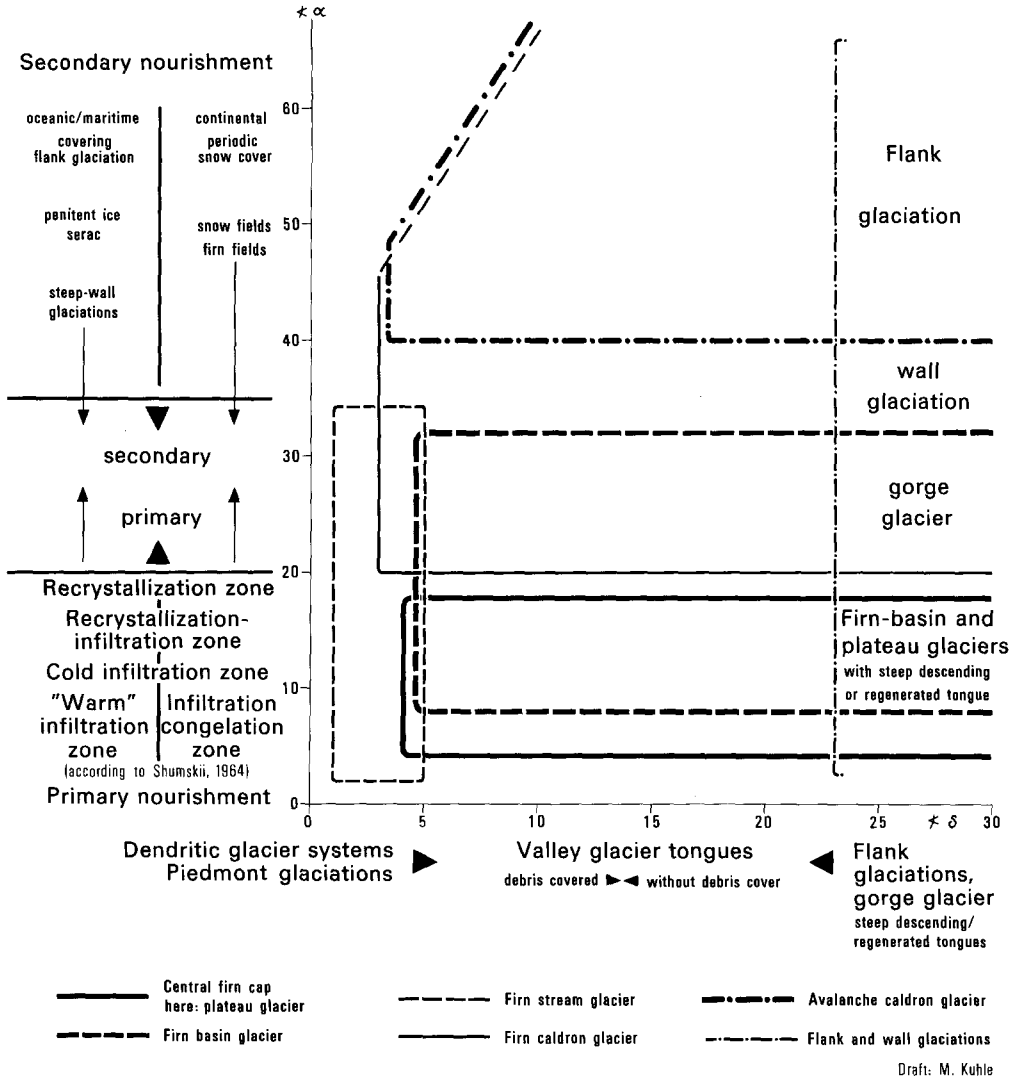

Fig 5
Idealized Glacier-typological scheme based on the angles α and δ

with debris and with average summit heights under 7000 m (since a distortion of the FED through, for example, outflowing or interrupted ablation zones in the same direction is expected, these phenotypically fully opposed types were placed in the same group).

Three scatter diagrams of the maximum, minimum, and mean factors of the equilibrium line deviation were drawn for each group (y-axis = FED; x-axis = $\alpha-\delta$), and a product-moment correlation after Pearson was done.

Group I, whose characteristics and number of value pairs (n=130) are best suited for answering the previous questions, had a correlation coefficient or $r^{xy}=0.916$ for the mean values (maxima r=0.915; minima r=0.898). The linear relationship of both random variables is thus highly significant. The measure of certainty B

$$\left(= \frac{\text{explained portion of variance}}{\text{total variance}}\right)$$

amounts to 0.84 for the mean values; i.e. 84% of the variance in the ELA deviation given by the empirical values is explained by the angle difference with linear regression (cf. Bahrenberg and Giese 1975, 149). This means that the remaining 16% of the variation can be traced back to the influence of the still unquantified distortional factors. Corresponding to a standard error of estimation (SEE) of 4.3, around 68% of the mean values lie in the range of ± 4.3 y of the average regression lines (Fig 3). The distance from the maximum and minimum regression lines to the mean regression line amounts to ± 2.15 y with a comparable SEE (max.=4.4 y; min. =4.8 y). Hence, 68% of the maximum/minimum value pairs (with an average interval of 4.3 y) are found within a range of around 13.5 y, and finally 95% of the mean values lie within ± 8.6 y of the accompanying regression line.

Group II, III, and IV clearly have a linear relationship between the variables (x/y), whereby the correlation coefficients are however generally lower, and the standard deviations higher:

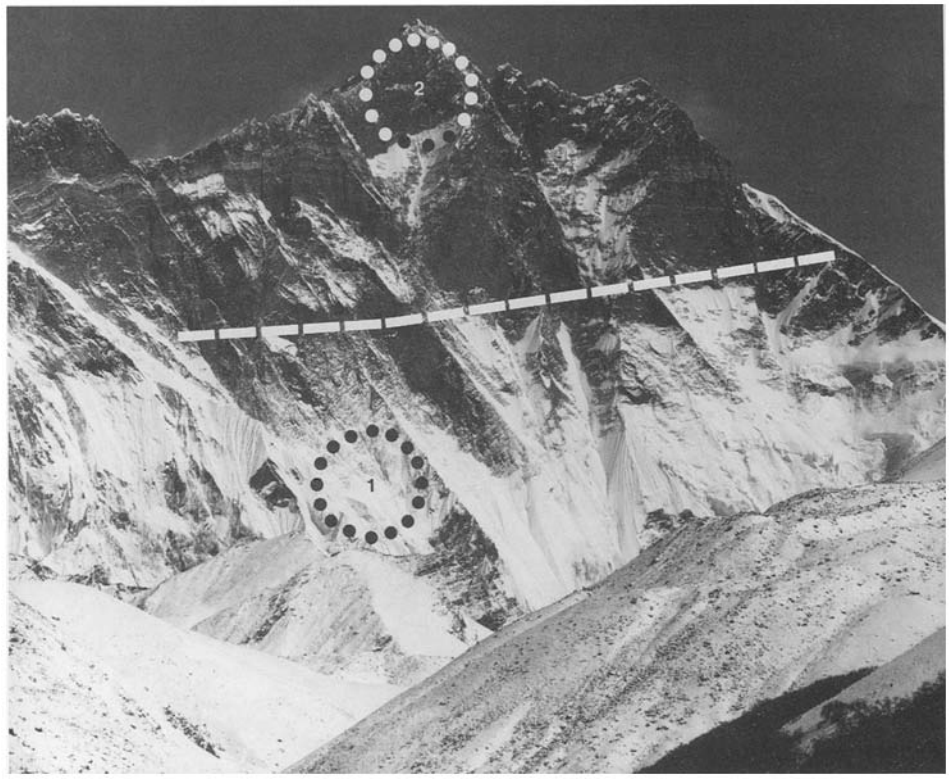

Fig 6
South face of the 8501-m-high Lhotse photographed from 4300 m asl. The 7.5-km-long wall section is located 27°57'N and 86°57'E in the Mahalangur Himalaya. Above 7100 m altitude glaciation ends, independent of the wall inclination. Only sporadic remains of the first winter snow, which extends down below the timberline, is able to cling to the steep wall surface composed of basset edges of metamorphic rock. The upper glacier boundary coincides with the 0° C line at 7100 m asl. The 0° C line was determined with 1800 telemetric infrared surface-temperature measurements in 1982 and 1984 on the summits in the Mahalangur Himal. Regression analysis with a correlation coefficient of $r_{xy} = -0{,}82$ yielded a boundary situated between c. 7000 m and 7200 m asl (dashed line). In the measured field at 6000–6125 m asl (dotted circle 1) surface temperatures of −0° to −4° C were measured under sunny weather conditions between 12°° and 13°° hours from Oct. 24 to Nov. 4, 1982, whereas at 8200–8500 m asl (dotted circle 2) temperatures of −16° to −38° C were measured. (Photo: Oct. 24, 1982, 12°° hours; M. Kuhle)

Mean values of Group II: r=0.74; SEE=5.4
Mean values of Group III: r=0.81; SEE=4.8
Mean values of Group IV: r=0.76; SEE=6.3

In addition, their gradients deviate from those of regression line I (Fig 3). Considering the unavoidable quantitative inhomogeneity of the group characteristics and the comparatively small number of value pairs, nothing else could have been expected. However, the theoretical presumptions are generally confirmed through the relative arrangement of the regression lines: (a) The regression line of the mean values of Group II (over 25% of the ablation zone covered with debris) clearly runs below those of Group I, i.e., with equal x-values lower y-values are intersected. (b) The regression line of Group III lies between those of I and II. The course above II first confirms the presumed effect of catchment areas over 7000 m, i.e., the relative increase in the y-values. The course below I shows contrarily that the positive shift of the mean values caused by the level of the catchment area is not capable of balancing or overcompensating the negative shift caused by the debris cover over 25% of the ablation area (see characteristics of Group III above).

Individual glaciers, however, with catchment areas around 8000 m attain or penetrate even the zone of the "normal glacier" (I) (cf. Fig 2d with b; with corresponding angle differences the Nuptse glacier with a catchment area at 7760 m alt. in spite of its 80% debris cover over the ablation zone has a slightly larger FED than the 5Y813C10 glacier with a bare tongue and a catchment area at 4868 m alt.) and are all characteristically above the accompanying (III) regression lines of the mean values, whereas the glaciers with catchment areas between 7000–7500 m alt. are found below. (c) The regression line for Group IV (outflowing or interrupted ablation areas) runs clearly above I, i.e., with equal x-values larger y-values are intersected.

Application of the factor of equilibrium line deviation to former glaciation

The calculation of equilibrium line deviations for subrecent glaciers must involve the reconstruction of three values: (a) the altitude of the glacier terminus, (b) the average summit elevation above the base value, and (c) the glacier level in the zone of the mathematical index (I_m). The last value is obtained from lateral moraine relicts, striation boundaries, or interpolation between both. With this information the horizontals b and e (Fig 1 and 2a) of the subrecent glacier can be determined. In calculating the equilibrium line deviation ($I_m - ELA$) it is advisable in the heuristic viewpoint to presume a variance spectrum of 8.6 (FED) units (Fig 3, screened zone). Thereby, at least the mean value and the average maximum and/or minimum range of variation of the subrecent position of the snowline is achieved with 68% probability. For glaciers which fall in one of

Fig 7
NNW face of 8848 m high Mt. Everest (Chomolungma, 27° 59' N/86° 56' E) photographed from the upper firn basin of the central Rongbuk Glacier at 6010 m asl. The snow and firn cover (◆) extending up to the foot of the wall at 6450 m asl belongs to the level at which snow transformation primarily occurs through the type of metamorphism close to the melting point. Within the lower 800 m (■■) of the NNW face of Mt. Everest as well, the seasonal, midday warmth leads to a snow-to-ice consolidation through settling, sintering, and ice formation between grains. This process allows snow, firn and ice to cling to the wall in spite of the steepness. Pressure compaction here is less than in the level firn basin. Above ca. 7000–7200 m altitude flank glaciation and glacier formation cease. The 0° C boundary is attained (cf. Fig 6), and mostly very low temperatures make the metamorphic processes, which occur at lower altitudes, impossible. Metamorphism through molecular diffusion of cold snow, as it occurs in the central plateau regions of Antarctica, requires the overburden pressure of thick snow accumulation and, thus, sufficiently long time. Here the relief makes this impossible, because the very cold and therefore physically dry snow is, at this altitude, not only shifted (as on the ice surfaces in Antarctica and Greenland) but also blown away. Only in stable lee positions, as in the Norton couloir, do seracs (×) over 100 m in thickness have a chance to form above 7200 m altitude. The snow and firn thicknesses necessary for glacier formation under extremely cold conditions accumulate on shallowly dipping rock ledges in the wind shadow. Whereas only slightly negative temperatures were recorded at the foot of the wall under sunny weather conditions in 1984, the author registered temperatures of −28° to −36° C at the summit (dotted circle) in September and October. Corresponding to prevailing westerly winds, the snow blown from the NNW and SSW faces of Mt. Everest toward the E does not contribute to the nourishment of the central Rongbuk and Khumbu glaciers. (Photo: Sept. 30, 1984, 16.30 hours; M. Kuhle).

the special groups II, III, and IV a rough but tendential estimation of the direction and amount of deviation is possible with the corresponding regression lines (Fig 3). Example: Suppose that the Hintereisferner (Ötztaler Alps) in its present form was the object in reconstructing a subrecent ELA. Using the regression line (I) of the mean values and its standard deviation (see above) the FED at an angle difference (I_g) of +5° 30' is 8.8 to −0.2 (cf. Fig 3; intersect. of +5° 30' with the upper and lower 68% line). Thereby, the former ELA can be calculated to be 2939–3045 m using

$$ELA = I_m - \frac{FED \cdot \text{vertical distance}}{100}$$

(the empirical value of the ELA, based on measurements between 1952/53 to 1974/75 is at 2950 to 3050 m; Kasser 1973; Müller 1977; Gross et al. 1977). The ratio of the range of variation of the reconstructed ELA of 106 m to the average vertical (1238 m) is 1:12.

On the other hand, when the area ratio method is applied in the same case without anticipating assumptions, e.g., concerning the climatic regime, which is not known in case of subrecent glaciers, at least AAR values between 0.5 and 0.8 would have to be assumed (Meier 1962, 70; Porter 1975). The ratio of the related variation in the ELA of 250 m (2770–3020 m; from Hoinkes 1970, Tab 2) to the average vertical of the glacier is, on the contrary, 1:5!

Glacier Typology Based on Surface Geometry

The proof that there is a significant correlation between glacier geometry and the ELA also evidences that topography is a fundamental element of glacial systems. The climatic parameters critical for the mass balances of glaciers belong to a relatively independent subsystem and can be analyzed independently, but are

insufficient for infering glaciers in their concrete manifestation. A system with which the glacier as a whole can adequately be described is first obtained at a higher level of integration by linking climatic parameters with topographical parameters. There are various approaches to typologically classify the variability in glaciers contingent on the specific topography. Among these are the relief-contingent classification of land ice (J. K. Charlesworth 1957), the digital glacier classification of UNESCO (1970), and the glacier typification by H. J. Schneider (1962), which is based on the form of the catchment area. In each of these cases, glaciers are classified based on formal criteria separating them into discrete groups. However, it is an essential point of this study to describe the continuous transition in topography, i.e., glacier geometry, which accompanies the primarily climate-induced expansion or retreat of a glaciation. This conception would correspond to the method of H. W. Ahlmann (1948) by which the different glacier configurations are quantified and made comparable to one another by plotting a so-called "normal curve" (= the vertical extension of a glacier is divided into 10 equal intervals on the absicessa, and the respective percentages of surface area are entered on the ordinate). This method has the disadvantage of being very time-consuming and presents the difficulty, especially for subrecent glaciations, of determining the exact surface area and contours.

Since the description of glacier geometry can be reduced to the angles α and δ, as has been proven sufficient with regard to equilibrium line deviation, it was checked whether this could also be used as a meaningful characterization of glaciers. To show the phenotypes, the localities of the 223 glaciers were each given signatures on the α/δ coordinates. These signatures (Tab 1, col. 3) correspond to the terminology of Schneider (1962): (1) central firn cap (Zf), (2) firn basin type (Fm), (3) firn stream (Fs), (4) firn caldron (Fk), (5) avalanche caldron (Lk), and flank glaciation/wall glaciation (Fl). (Schneider's ice stream system (7) did not prove to be distinguished, since it represents a more quantitative than a qualitative variation of the firn stream type (3); Schneider 1962, 281). When two types of nourishment appear to participate equally in the formation of a glacier, this would be marked with the corresponding combination of symbols (Fig 4).

The distribution of glacier symbols in the α (y-axis)/δ (x-axis) diagram has two basic attributes (Fig 4): (1) the individual types form coherent groups with clear concentration zones, and (2) no one type has a numerically exclusive range – all zones are overlapped on the periphery by other groups. The empirical continuity of types, which exhibits successive quality differences, is thereby adequately substantiated. An attempt at schematizing this in an idealized way through extrapolation of the values on hand is made in Fig 5. (The zone of the central firn cap consists here only of values from plateau glaciers with outlet tongues.

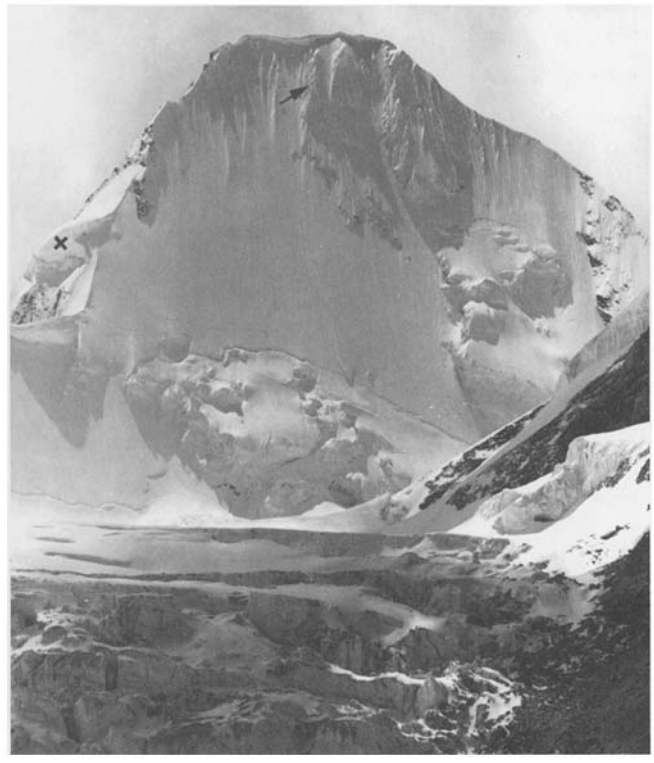

Fig 8 ENE face of the 6714 (6697)-m-high Lingtrentse (28°02'N/86°51'E) photographed from the central Rongbuk Glacier. Independent on the exposure to the wind, as the view of the S face with a serac (×) which has a greater exposure to the wind shows, the 6000 to 7000 m high summits are covered with flank glaciations. The extreme steepness of the walls evidence the meaningless of the degree of inclination for the ice cover at this altitude; the temperatures drop below freezing sufficiently often so that adhesion to the rock and metamorphism of new snow are possible (in contrast, cf. Fig 6, 7). Avalanche tracks and the flowage of seracs substantiate that the central Rongbuk Glacier is nourished by this wall. Up to an altitude of c. 7000–7200 m, the steep faces in the Mt. Everest region contribute largely to glacier nourishment. Snowfall and hoar-frost also add to flank glaciation at this altitude. This is shown by the formation of ribbed firn (→) on the upper 120 m of the wall. (Photo: Sept. 24, 1984, 14.20 hours; M. Kuhle).

According to definition, however, continental glaciations also belong to this type (Schneider 1962). Taking them into account would presumably effect an expension of the Zf zone into that of the Fs type up to a δ of 1°). It is to be mentioned here that the overlapping zones are mainly composed of transitional types – which cannot be defined as one or the other since the transition is continous – or are composed of glaciers of one type containing at least some elements of another type – for example, obvious firn caldron components are linked to an obvious firn stream glacier. Specifying data on the characteristics of the accumulation and ablation areas were able to be related to the absolute values of the angles α and δ. Up to an angle of $\alpha = 20°$ primary glacier nourishment can be regarded as predominant. Between 20° and 35° a proportionally increasing mixture

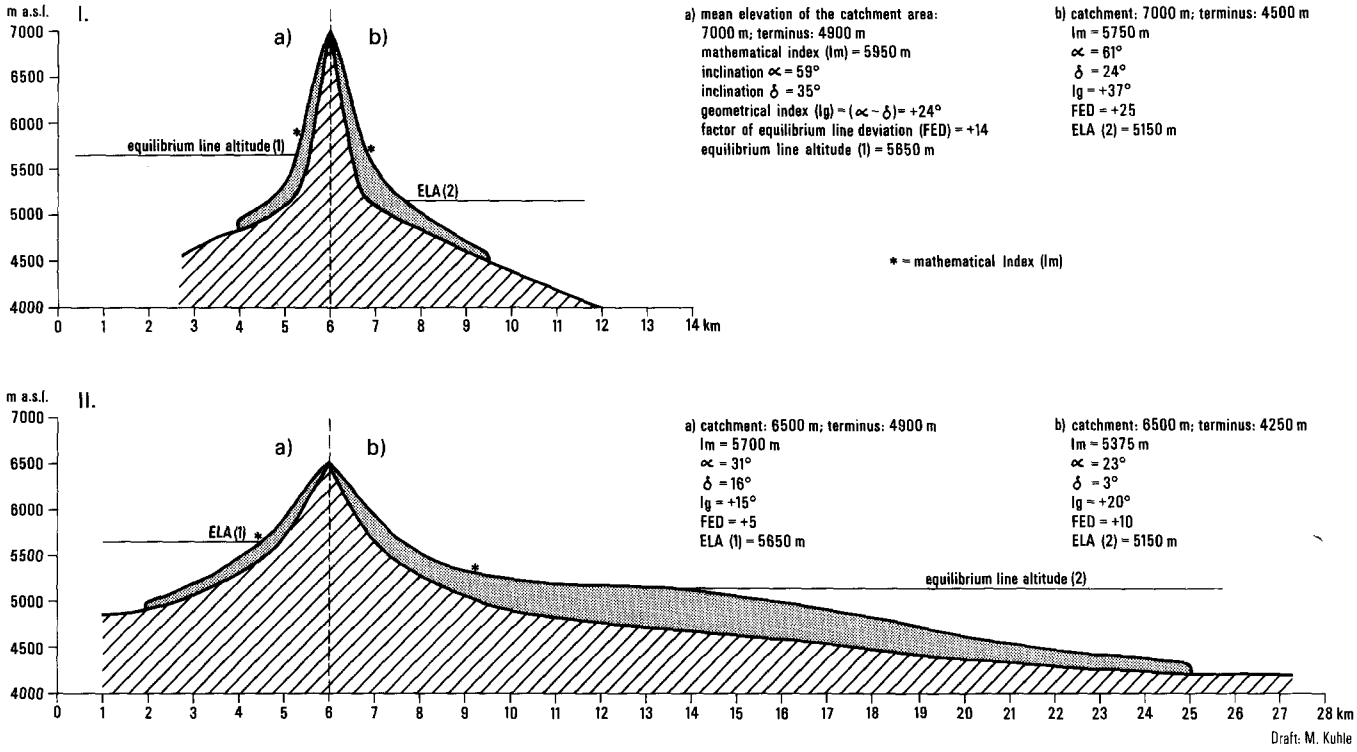

Fig 9 Dependency of the intensity of glaciation on topography: I corresponds to the relief of the main chain of the Himalayas, II to the relief within the central Tibetan plateau. Under equal climatic conditions the glacier termini of Ia and IIa reach the same altitude although the feeding ground of Ia is 500 m higher; this can be put down to the smaller accumulation capacity of the steeper feeding ground of Ia (α = 59°). When reducing the ELA by 500 m Ib only reaches 4500 m while IIb flows down to 4250 m. The FED was calculated using regression line I (Fig 3).

with secondary nourishment is characteristic. Above 35° the former decreases to the advantage of the latter. The classification of thermodynamic ice formation processes worked out by Shumskii (1964, Fig 122) is interesting here insofar as phenomenological differences in numerically identic glaciers can also be explained with the related differentiation in maritime/oceanic and continental zones. Thus, regarding the firn caldron type, for example, steep walls in an oceanic climate can be occupied by thick flank ice, seracs, and wall ice flowing down into gorges (Fig 8), whereas in continental climates only thin snow and firn fields are observed, or at very high absolute altitudes the walls extend up into the recrystallization zone and are thus only periodically covered with snow (Fig 6 and 7; Kuhle 1986b).

In comparison, the δ values allow an evaluation of the configuration of the tongue – but here as well the given boundaries (Fig 5, x-axis) are only to be understood as major tendencies along a continous transition.

Topography and Climate-Elements of a Glacial Feedback System

Shifting of the topographic setting of glaciers is primarily caused by climatic changes and thus proceeding expansion or retreat of the ice body. However, the linkage between climatic and topographic parameters is not dominated by one or the other but acts in the way of a true feedback system (cf. Ashby 1964). The amount of increase in surface area evoked by an initial lowering of the ELA is the decisive factor for the effect which topography has on the climate. On the S slopes of the Himalayas, for example, an ELA depression of 500 m still remains within the zone of high relief and thus effects a comparatively slight enlargement of the catchment areas and no significant change in glacier geometry (Fig 9 I a–b). In Central Tibet, however, such an ELA depression of 500 m causes the small steep alpine glaciers to reach the level of the high plateau where they build up coalescing piedmont glacier lobes (Fig 9 II a–b) and finally an inland ice sheet (cf. Kuhle 1986a, 1987 and this volume). The very small recent glaciation of the Tibetan plateau as compared to that one of the Alps resulted in the view that the glaciation of Tibet did only increase as insignificantly during the Pleistocene and fell behind in relation to the glaciation of the Alps; the reason being the aridity (v. Wissmann 1959). Due to the influence of topography, however, similar climatic conditions can result in very different intensities of glaciation, as is shown in Fig 9. Thus, topographical parameters are of the same influence on glacial formation as are climatic

parameters. Therefore, differences in the actual and former dimensions of glaciations do not necessarily depict solely climatic but also topographical differences and variations. Topographically induced enlargement of a glacier has climatic consequences though: the Tibetan debris and rock surfaces, which presently absorb 80% of the solar radiant energy and thus heat up the atmosphere, changed during the Pleistocene glaciation into cooling surfaces by reflecting 95% of the energy. The induced negative shift of temperature leads once again to a lowering of the ELA and a further expansion of the glaciated area. (The 2–2.4 million km^2 inland glaciation of Tibet was apparently build up by this kind of a self-boosting process. Due to the subtropical situation in the case of extreme radiation transparency in the atmosphere at great altitudes where the irradiation is three to four times more than in higher latidudes the impact on the earth's thermal balance was so severe that the Tibetan ice sheet induced the onset of the ice age (Kuhle 1986a, 1987 and this volume).

It can be generally said that the surface effectiveness of a shift in the ELA is all the greater, the smaller the values are, which the angles α and δ in glacier geometry have. The concrete effect that the topographically controlled surface growth has on the climate is, on the other hand, determined by the altitude above sea level and latitude as a function of the solar radiant energy.

Conclusions

A regular interdependency between glacier geometry and mass balance is proven by the highly significant correlation between the geometrical glacier index (I_g) and the factor of equilibrium line deviation FED. Particularly concerning paleoglaciers which are only accessible in their entirety, glaciers must thus be treated as complex systems whose fundamental components contain both climatic and topographic parameters. To be able to purely climatically interpret regional and temporal shifts in the ELA the distorting influence of the specific topographical setting must hence be excluded. This has not previously been done when using the customary methods for approximately calculating the ELA. The accuracy achieved when calculating equilibrium line deviation affected by the heterogenous glacier geometry depends on the number of value pairs used in the investigation. Through the increasing availability of long-term mass balance data and the production of large scale glacier maps the accuracy of predications will improve further. The expansion and retreat of glaciations is accompanied by a continous change in the topographical setting. The variations of glacier geometry which are quantitatively given on the α/δ coordinate axes (Fig 6) indicate (a) a change in the factor of equilibrium line deviation and (b) that identical amounts of shift in the ELA cause differing amounts of change in the surface of catchment areas depending on whether the shift in the ELA occurs in an area with high or low relief (Fig 9). Since a change from rock and debris surfaces to permanent snow cover induces a significant change in the atmospheric temperature balance, the variability in glacier geometry has a distinct effect on the climate. The impact on the climate increases at identic surface areas dependent upon the solar radiation with altitude above sea level, and with low latitudes. The investigation of the feedback between topographical and climatic parameters of glacial systems in their respective global positions appears to be of fundamental importance in understanding paleoclimatic evolution (Kuhle 1986a, 1987 and this volume).

References

Ahlmann, H. W. son: Glaciological Research on the North Atlantic Coasts. Royal Geographical Society London, Research Series 1, 83 (1948)

Andrews, J. T.: Glacial systems. An approach to glaciers and their environments. Duxbury Press, North Scituate, MA 1975.

Andrews, J. T.; Miller, G. H.: Quaternary history of northern Cumberland Peninsula, Baffin Island, N.W.T., Canada: Part IV: Maps of the present glaciation limits and lowest equilibrium line altitude for north and south Baffin Island. Arctic and Alpine Research 4, 1, 45–59 (1972)

Ashby, W. R.: An Introduction to Cybernetics. Methuen, New York 1964.

Braithwaite, R. J.; Müller, F.: On the parameterization of glacier equilibrium line altitude. World Glacier Inventory, IAHS–AISH Publ. No. 126, 263–271 (1980)

Brückner, E.: Die Hohen Tauern und ihre Eisbedeckung. Zeitschrift des Deutsch-Östereichischen Alpenvereins 17, 163–187 (1886)

Brückner, E.: Die Höhe der Schneelinie und ihre Bestimmung. Meteorologische Zeitschrift 4, 31–32 (1887)

Charlesworth, J. K.: The Quaternary Era. London 1957.

Drygalski, E. v.; Machatschek, F.: Gletscherkunde. Enzyklopädie der Erdkunde. Wien 1942.

Enquist, F.: Der Einfluß des Windes auf die Verteilung der Gletscher. Bulletin of the Geological Institute, Uppsala, 14, 1–108 (1916)

Finsterwalder, R.: Wissenschaftliche Ergebnisse der Alai-Pamir Expedition. Teil 1. Geodätische, topographische und glaoziologische Ergebnisse, 1, Berlin 1932.

Finsterwalder, R.: Gletschergeschwindigkeitsmessungen und gletscherkundliche Bemerkungen. In: Bauer, P. Um den Kantsch, 141–143, München 1933.

Finsterwalder, R.: Die geodätischen, gletscherkundlichen und geographischen Ergebnisse der Deutschen Himalaya-Expedition 1934 zum Nanga Parbat. Teil II: Gletscherkunde, 106–157, Berlin 1938.

Finsterwalder, R.: Die zahlenmäßige Erfassung des Gletscherrückganges an Ostalpengletschern. Zeitschrift für Gletscherkunde und Glazialgeologie 2, 2, 189–239 (1953)

Flint, R. F.: Glacial and Quarternary Geology. John Willy & Sons, New York 1971. (Chs. 4, 18)

Gross, G.; Kerschner, H.; Patzelt, G.: Methodische Untersuchungen über die Schneegrenze in alpinen Gletschergebieten. Z. f. Gletscherkunde u. Glazialgeologie 12, 2, 223–251 (1977)

Hawkins, F.: Equilibrium-line altitudes and paleoenvironment in the Merchants Bay area, Baffin Island, N.W.T., Canada. Journal of Glaciology 13, 109, 205–213 (1985)

Hermes, K.: Der Verlauf der Schneegrenze. Geographisches Taschenbuch 1964/65, 58–71, Wiesbaden 1965.

Heuberger, H.: Beobachtungen über die heutige und eiszeitliche Vergletscherung in Ost-Nepal. Z. f. Gletscherkunde u. Glazialgeologie 3, 349–364 (1956)

Heuberger, H.: Die Schneegrenze als Leithorizont in der Geomorphologie. In: Höhengrenzen in Hochgebirgen; Arb. a. d. Geograph. Inst. d. Univ. d. Saarlandes 29, 35–48 (1980)

Höfer, H. v.: Gletscher- und Eiszeitstudien. Sitzungsber. d. Akad. d. Wiss. Wien, Math.-Nat. Kl. 1, 79, 331–367 (1879)

Hoinkes, H.: Methoden und Möglichkeiten von Massenhaushaltsstudien auf Gletschern. Ergebnisse der Messreihe Hintereisferner (Ötztaler Alpen) 1953–1968. Zeitschrift für Gletscherkunde und Glazialgeologie 6, 1/2, 37–90 (1970)

Jiresch, E.: Die geodätischen und kartographischen Arbeiten am Untersulzbachkees (Venedigergruppe) von 1974 bis 1982. In: Glaziologie u. Kartographie; W. Pillewizer Festschrift. Geowiss. Mitt. 21, 67–112, Wien (1982)

Kasser, P.: Fluctuations of Glaciers 1959–1965. A contribution to the IHD. IASH (ICSI)-UNESCO, Louvain 1967.

Kasser, P.: Fluctuations of Glaciers 1965–1970. IAHS (ICSI)-UNESCO, Paris 1973.

Kuhle, M.: Der Dhaulagiri- und Annapurna-Himalaya. Ein Beitrag zur Geomorphologie extremer Hochgebirge. Zeitschrift für Geomorphologie, Supplement Bd. 41, 1–229 (1982)

Kuhle, M.: Die Vergletscherung Tibets und die Entstehung von Eiszeiten. Spektrum der Wissenschaft 9, 42–54 (1986a)

Kuhle, M.: The Upper Limit of Glaciation. GeoJournal 13, 4, 331–346 (1986b)

Kuhle, M.: Subtropical Mountain- and Highland-Glaciation as Ice Age Triggers and the Waning of the Glacial Periods in the Pleistocene. GeoJournal 14, 4, 393–421 (1987)

Kurowski, L.: Die Höhe der Schneegrenze mit besonderer Berücksichtigung der Finsteraarhorngruppe. Geographische Abhandlungen 5, 1, 115–160 (1891)

Lichtenecker, N.: Die gegenwärtige und die eiszeitliche Schneegrenze in den Ostalpen. Verhandl. d. III. Intern. Quartär-Konferenz, Wien 1936, 141–147, 1938.

Louis, H.: Schneegrenze und Schneegrenzbestimmung. Geographisches Taschenbuch 1954/55, 414–418, 1955.

Meier, M. F.: Mass budget of South Cascade Glacier, 1957–60. U. S. Geol. Survey Prof. Paper 242–B, 206–211 (1961)

Meier, M. F.; Post, A. S.: Recent variations in mass net budgets of glaciers in western North America. Commission of Snow and Ice Symposium of Obergurgl 1962. IASH, Publ. 58, 63–77 (1962)

Meier, M. F.; Tangborn, W.: Net budget and flow of South Cascade glacier, Washington. Journal of Glaciology 5, 41, 547–566 (1965)

Müller, F.: Inventory of glaciers in the Mount Everest region. In: Perennial Ice and Snow masses, 47–59; UNESCO Technical Papers in Hydrology 1 (1970)

Müller, F.; Caflisch, T.; Müller, G.: Firn und Eis der Schweizer Alpen. Gletscherinventar. Geogr. Inst., ETH Zürich, Publ. 57, 1976.

Müller, F.: Fluctuations of Glaciers 1970–1975. IAHS (ICSI)-UNESCO, Paris 1977.

Müller, F.: Present and late Pleistocene equilibrium line altitudes in the Mt. Everest region – an application of the glacier inventory. In: World Glacier Inventory, IAHS-AISH Publ. 126, 75–94, 1980.

Østrem, G.: The height of the glaciation limit in southern British Columbia and Alberta. Geogr. Annaler, Ser. A, 48, 126–138 (1966)

Partsch, J.: Die Gletscher der Vorzeit in den Karpathen und den Mittelgebirgen Deutschlands. Breslau 1882.

Porter, S. C.: Quaternary glacial record in Swat Kohistan, West Pakistan. Bull. Geol. Soc. Am. 81, 1421–1446 (1970)

Porter, S. C.: Glaciological evidence of climatic change. In: Wigley, T. M. L.; Ingram, M. J.; Farmer, G., (eds.) Climate and history studies in past climates and their impact on man. Cambridge 1981.

Richter, E.: Die Gletscher der Ostalpen. J. Engelhorn, Stuttgart 1888.

Schneider, H.-J.: Die Gletschertypen. Versuch im Sinne einer einheitlichen Terminologie. Geographisches Taschenbuch, 276–283, Wiesbaden 1962.

Schytt, V.: Mass balance studies in Kebnekajse. Journal of Glaciology 4, 33, 281–286 (1962)

Sharp, R. P.: Accumulation and ablation on the Seward-Malaspina Glacier system, Canada-Alaska. Geol. Soc. Am. Bul. 62, 726–744 (1951)

Shumskii, P. A.: Energiia oledeneniia i zhizn lednikov (Energy of glacierization and the life of glaciers). Geografgiz, Moscow 1947; transl. by W. Mandel, The Stefansson Libary, New York 1950.

Shumskii, P. A.: Principles of Structural Glaciology. translated from the Russian by D. Kraus; Dover Publ., Inc., New York 1964.

UNESCO/IASH: Perennial ice and snow masses. A guide for compilation and assemblage of data for a world inventory. Technical Papers in Hydrology 1, 1–59 (1970a)

UNESCO/IASH: Perennial ice and snow masses. A contribution to the International Hydrological Decade. Technical Papers in Hydrology, Paris (1970b)

Visser, P. C.: Wissenschaftliche Ergebnisse der Niederländischen Expeditionen in den Karakorum und die angrenzenden Gebiete in den Jahren 1922–1935. Vol. II, Glaziologie, 1–216, 1938.

Walcher, J.: Nachrichten von den Eisbergen in Tirol. Wien 1773.

Wang Yinsheng; Qiu Jiaqi: Distributive Features of the Glaciers in Bogda Region, Tian Shan. Journ. of Glaciology and Cryopedology 5, 3, 17–24 (1983)

Wissmann, H. v.: Die heutige Vergletscherung und Schneegrenze in Hochasien mit Hinweisen auf die Vergletscherung der letzten Eiszeit. Akad. d. Wiss. u. d. Lit., Abh. d. math.-nat. wiss. Kl., No. 14, 1103–1407. Mainz 1959.

Wu Guanghe; Zhang Shunying; Wang Zhongxiang: Retreat and Advance of Modern Glaciers in Bogda, Tian Shan. Journ. of Glaciology and Crypedology 5, 3, 143–152 (1983)

Young, G. J.: Accumulation and ablation patterns as functions of the surface geometry of a glacier. Snow and Ice- Symposium, Proceedings of the Moscow Symposium, August 1971, IAHS-AISH Publ. 104, 134–138 (1975)

Zhang Xiangsong; Chen Jinming; Xie Zichu; Zhang Jinhua: General features of the Batura glacier. Professional Papers on the Batura Glacier, Karakoram Mountains, 8–27, 1980.